

Complementary use of multi-model climate ensemble and Bayesian Model Averaging for projecting river hydrology in the Himalaya

Shafkat Ahsan

University of Kashmir

M. Sultan Bhat

University of Kashmir

Akhtar Alam (✉ alamakhtar@uok.edu.in)

University of Kashmir

Hakim Farooq

University of Kashmir

Hilal A. Shiekh

University of Kashmir

Research Article

Keywords: Climate change, Jhelum basin, RCP, Water balance, SWAT model, multi-model ensemble, BMA

Posted Date: July 22nd, 2022

DOI: <https://doi.org/10.21203/rs.3.rs-1850139/v1>

License:  This work is licensed under a Creative Commons Attribution 4.0 International License.

[Read Full License](#)

1 **Complementary use of multi-model climate ensemble and Bayesian Model Averaging for**
2 **projecting river hydrology in the Himalaya**

3 *Shafkat Ahsan¹, M. Sultan Bhat¹, Akhtar Alam^{2*}, Hakim Farooq¹, Hilal A. Shiekh¹,*

4 *¹Department of Geography and Disaster Management, University of Kashmir, Srinagar 190006,*
5 *India.*

6
7 **Correspondence author: alamakhtar@uok.edu.in*
8

9 **Abstract**

10 This study aims to predict the hydrology of the Jhelum basin under changing climatic scenarios
11 based on Representative Concentration Pathways (RCPs). Six Global Circulation Models were
12 dynamically downscaled for reliable climatic projections over the 21st century (2020-2080). To
13 reduce the uncertainty associated with climate projections, multi-model ensemble estimations
14 were refined using Bayesian Model Averaging (BMA). The assessment reveals that compared
15 to the baseline (1980-2010) values, the annual mean maximum temperature in the basin will rise
16 by 0.41–2.31°C and 0.63–4.82°C and the mean minimum temperature will increase by 1.39–2.37
17 °C and 2.14–4.34 °C under RCP4.5 and RCP8.5 respectively. While as, precipitation is expected
18 to decrease by 7.2–4.57% and 4.75–2.47% under RCP4.5 and RCP8.5 correspondingly. BMA
19 ensemble projections were used in the Soil and Water Assessment Tool (SWAT) to simulate the
20 future hydrological scenarios of the drainage basin. With the changing climate, the discharge of
21 rivers in the Jhelum basin is expected to witness reductions by about 23–37% for RCP4.5 and
22 19–46% for RCP8.5. Moreover, the water yield of the basin may also exhibit decreases of 17–
23 25% for RCP4.5 and 18–42% for RCP8.5. The projected scenarios are likely to cause water
24 stress, affect the availability of water for diverse uses, and trigger transboundary water sharing
25 related conflicts. The impact of climate change on discharge demands early attention for the
26 development of mitigation and adaptive measures at the regional level and beyond.

27 **Keywords:** *Climate change, Jhelum basin, RCP, Water balance, SWAT model, multi-model*
28 *ensemble, BMA.*

29 **1. Introduction**

30 Changing climatic regimes and their impact on water resources have attracted considerable
31 attention in the contemporary world because of its tremendous environmental and socioeconomic
32 implications (Jasper et al., 2004; Luo et al., 2019; Reshmidevi et al., 2018). Mounting evidence
33 exists about the impact of increase in global mean temperatures on regional water budget
34 (Huntington, 2006). Moreover, changing precipitation patterns and evapotranspiration rates
35 projected under the climate change scenarios will further alter the hydrological
36 systems (Kundzewicz et al., 2008; Raneesh & Santosh, 2011). Therefore, while devising effective
37 water management policies and adaptation strategies to offset the climate change induced
38 stresses, it becomes quintessential to evaluate the hydrological responses and sensitivity of the
39 riverine systems to the changing climate (Bhatta et al., 2019; Reshmidevi et al., 2018; Rodrigues
40 et al., 2020).

41 Multiple studies have assessed the hydrological imprints to changing climate across the different
42 river basins of the world (Bajracharya et al., 2018; Hao et al., 2018; Liu et al., 2011; Luo et al.,
43 2019; Reshmidevi et al., 2018; Rodrigues et al., 2020; Tan et al., 2017; Vetter et al., 2017; Yu et
44 al., 2018). Global circulation models (GCM) are the popular tools in use for projecting climate
45 change under different emission scenarios. However, GCMs provide information on a coarse-
46 scale with large grid sizes and insufficiently capture the regional heterogeneity that impact the
47 hydrological processes on the basin scale. Regional climate models (RCMs) with a finer grid size
48 have been developed to improve the outputs of GCMs. Although RCMs perform better in
49 simulating the local climate; however, inherit significant error/bias from GCMs (Chen et al.,
50 2013). As a result, using the RCM outputs directly into the hydrological models can yield
51 significant deviations in the model outputs with respect to the observed data (de Oliveira et al.,
52 2017). As a result, prior to any hydrological simulations, bias adjustment of the raw RCM results
53 is critical (Luo et al., 2019). “Coupled Model Intercomparison Project Phase 5 (CMIP5)” GCMs
54 provide the outputs based upon the Representative concentration pathways (RCPs) that describe
55 the net radiative forcing levels till 2,100 ranging from a mitigating pathway (RCP2.6),

56 mediumstabilizing pathways (RCP4.5/RCP6), and extreme climatic pathway
57 (RCP8.5)(Meinshausen et al., 2011; Taylor et al., 2012).

58 GCM output carries a substantial amount of uncertainty with it and must be taken in
59 cognizance while carrying any impact assessment studies. The cascade of uncertainty is nestled
60 in the range of socioeconomic or developmental pathways that the world may take in the future;
61 incomplete knowledge or representation of the climatic system and its interactions; and the
62 structural or the parametric differences in the GCMs. As such, the results from the single model
63 must be interpreted with caution (Reshmidevi et al., 2018). To this end, ensemble projections
64 have been proposed on account of their reliability and uncertainty assessment (Khan et al.,
65 2021). In comparison to the outputs from separate models, the multi-model ensemble has
66 demonstrated to be more effective in the representation and simulation of climatic variables
67 (Gleckler et al., 2008; Knutti et al., 2010; Zhang & Huang, 2013). The ensemble techniques can
68 vary from the simple arithmetic ensemble mean wherein each model is weighted equally
69 irrespective of its performance, to the weighted ensemble mean. BMA is a weighted ensemble
70 method in which the relative competence of models is determined and model weights are
71 optimized so that BMA ensemble projections closely match the observed data (Massoud et al.,
72 2020). In this way, higher weights are applied to more skillful models as compared to low
73 skillful models. BMA has been previously used for developing ensemble projections in
74 studies like Huang, (2014), Khan et al., (2021), and Massoud et al., (2020).

75 Generally, hydrological models forced with climatic scenarios have been employed
76 to simulate the possible implications on the stream flows, catchment storage, and other water
77 balance components. Different hydrological models that can replicate the hydrological properties
78 and processes operating within a basin have already been developed (Krysanova & Hattermann,
79 2017). Soil and Water Assessment Tool (SWAT), is being widely used for evaluating the
80 likely implications of changing climatic regimes on hydrological processes (Bajracharya et al.,
81 2018; Bhatta et al., 2019; Rodrigues et al., 2020; Narsimlu et al., 2013; Touseef et al., 2021).

82 Climate change's potential implications are more noticeable in the mountainous regions
83 like Himalayas, particularly on water resources, where snowmelt and glacial ice melt are the
84 major determinants of streamflow (Viviroli et al., 2007; Lutz et al., 2014; Immerzeel et al.,
85 2013). Significant increases in the temperature along with the declining precipitation patterns
86 have been reported for Jhelum basin (Ahsan et al., 2021a, b). Having established climate change

87 signals, it becomes obvious that the water resources will be most affected in this region. The
88 imprints of the observed climatic variability are already visible over the hydrological regime of
89 the Jhelum basin. For example, climate change is putting a lot of strain on the aquatic systems in
90 the region (Alam et al., 2020). Lone et al., (2021) reported significant decreasing trends in the
91 streamflow, driven by observed climate variability. Hence, climatic changes are likely to further
92 impact the water security of the region and challenge the existing management strategies. The
93 hydrological consequences of the climatic changes can transmit to the overall prosperity of the
94 region due to dependence of other sectors viz., irrigation, domestic, industrial, tourism, and
95 hydropower generation on the water resource base. Limited studies have been attempted so far in
96 the Jhelum basin that project the hydrological responses of changing climate e.g., Singh Jasrotia
97 et al., (2021). However, key limitations with this study are that it uses outputs of a single RCM
98 and lacks any detailed assessment of water balance components. Hence, it is imperative to have a
99 rigorous quantification of the hydrological responses to the projected changes in climatic
100 regimes. For this purpose, the current study utilizes outputs from 6 GCMs under a medium
101 stabilizing pathway (RCP4.5), and an extreme pathway (RCP8.5). The study primarily aims to
102 develop the robust climatic projections for the 21st century, using the multi-model ensemble based
103 on Bayesian model averaging framework. The study subsequently employs the hydrological
104 model SWAT coupled with the climatic scenarios to project the changes in the streamflow and
105 different components of water balance over the 21st century. No such comprehensive study has
106 been attempted yet for the Jhelum basin; the present one can thus serve as a benchmark study
107 while planning for the mitigation of hydrological implications ascribed to climate change and pave
108 the way for formulation of adaptive policy for sustainable water management.

109 **2. Study area**

110 The present study is attempted for Jhelum basin (Fig 1) located in the lap of Himalaya with an area
111 of about 15000 km². The trunk stream, Jhelum constitutes an important tributary of the Indus River
112 system forming an elongated bowl-shaped basin that originated from the collision between Indian
113 and Eurasian plates (Alam et al., 2015, 2017). Based on stratigraphy and elevation, the basin can
114 be divided into 3 major physiographic divisions viz., mountainous uplands, extensive plateaus of
115 lacustrine deposits (Karewas), and valley floor with the numerous streams draining into
116 Jhelum (Bhat et al., 2018). The region's climatic regime is controlled by two distinct weather

117 patterns viz., Western Disturbance in winter months and southwest Monsoons in the summer half.
118 The impact of the latter is somewhat limited and the major proportion of the precipitation is
119 received in the winter months, mainly in the form of snowfall. The winter precipitation feeds the
120 glaciers and acts as a buffer in maintaining the streamflow of the river Jhelum during the dry
121 periods. The climate of the region is moderate; however, the annual temperature variations of the
122 region range from sub-freezing during the winter and can be as high as 35 °C during the summer.
123 The region supports a population of ~7 million persons with heavy reliance on water resources
124 for sustenance.

125 **3. Materials and methods**

126 *3.1 Observed hydroclimatic data*

127 Observed climate data (1980-2016) for temperature and precipitation variables at a daily scale
128 was procured from the Indian meteorological department, regional office Srinagar, J&K India.
129 This data was utilized for the bias correction of the GCM data and also as input for the baseline
130 run of the SWAT model. For the other SWAT input climatic variables i.e., Relative Humidity,
131 Wind Speed, and Solar Radiation, “Climate Forecast System Reanalysis (CFSR)” data were used.
132 The observed streamflow data for the 3 gauges on the trunk stream viz., Sangam, Asham, and
133 Ram Munshi Bagh were used. Streamflow data was used in calibrating and validating the SWAT.

134 *3.2 Climate scenario projections*

135 The Coordinated Regional Climate Downscaling Experiment (CORDEX) was developed under
136 the aegis of the World Climate Research Programme to stimulate climatic scenarios and improve
137 regional impact assessment. CORDEX over the south Asian domain provides data for multiple
138 GCM-RCM combinations at a grid size of 0.44° (~50 km). CORDEX-SA has previous successful
139 applications in the Himalayan region e.g., (Dimri et al., 2018; Krishnan et al., 2019). A total of
140 6 GCMs (Table 1) downscaled dynamically using the RegCM4 RCM (Giorgi et al., 2012) were
141 used in the projection of the climatic scenarios under RCP4.5 and RCP8.5. The projected span
142 (2006-2099) was split into 3 periods viz., 2011-2040 referred in the manuscript as 2020s, 2041-
143 2070 referred in the manuscript as 2050s, and 2071-2099 referred in the manuscript as 2080s. The
144 relative changes in mean climatology over the different spans of 21st century was computed from
145 the baseline (1980-2010) climatology.

146 3.3 Bias-correction of GCM/RCM data

147 Prior to using the GCM/RCM data for the projection of climatic changes or its hydrologic
148 implications, it is necessary to apply the bias correction techniques because the data obtained
149 from the climate models inherit systematic biases(Luo et al., 2019). A wide range of bias-
150 correction techniques have been devised(Teutschbein& Seibert, 2012); and in the present study
151 Variance Scaling (VS) was used for biascorrecting the temperature data, while a hybrid of power
152 transformation (PT) and local intensityscaling (LOCI) techniqueswas employed for bias
153 correcting the precipitation data.

154 Variance scaling is an effectivetechnique and has the advantage of correcting both the mean and
155 variance (Teutschbein& Seibert, 2012).Power transformation of the precipitation data also
156 corrects both mean and variance in the raw data. However, the limitation of the PT method is
157 that it doesn't correct the wet day frequency. Hence before its use, the wet day frequency is
158 adjusted using the local intensity scaling method. The details of thesebias correction techniques
159 are given inFang et al., (2015).To check the skill and efficiency of the RCM simulations, RCM
160 data (raw and bias-corrected) were compared with observational data on monthly time series
161 using the efficiency indicators like Coefficient of determination(R^2), percentage bias(PBIAS)
162 and Nash Sutcliffe efficiency (NSE). R^2 given by Eq.1 is a measure of goodness-of-fit among the
163 observed and model data ranging between0and1. R^2 values nearing 1 imply a higher agreement
164 among observed and model values. PBIAS (Eq.2) measures the model data's mean tendency to
165 be greater or lesserthan actual observations. PBIAS has an optimum value of 0 with positive
166 valuesdepicting underestimation and negative values depicting overestimation in model
167 simulations.NSE is a standardized statistic (Eq.3) that measures deviations among the modeled
168 and observed data normalized by the observational data variance (Takele et al., 2021).It values
169 between $-\infty$ to 1 and $NSE = 1$ depicts modeled data are equal to that of the observed data(Nash &
170 Sutcliffe, 1970).

171

$$R^2 = \frac{\sum_{i=1}^n (O_i - \bar{O})(M_i - \bar{M})}{\sqrt{\sum_{i=1}^n (M_i - \bar{M})^2 \sum_{i=1}^n (O_i - \bar{O})^2}} \quad (1)$$

172

$$PBIAS = \frac{\sum_{i=1}^n (O_i - M_i) \cdot 100}{\sum_{i=1}^n (O_i)} \quad (2)$$

173

$$NSE = 1 - \frac{\sum_{i=1}^n (O_i - M_i)^2}{\sum_{i=1}^n (O_i - \bar{O})^2} \quad (3)$$

174

175 Where, O_i are the observational data values and M_i are the model simulated values.

176 *3.4 Bayesian model averaging (BMA) for multi-model Ensemble*

177 On account of parametric and structural differences, GCMs/RCMs produce different
 178 outputs(Wallach et al., 2016). Hence, a single climate model's output may still be subject to
 179 uncertainty (Uusitalo et al., 2015).The bias-corrected RCM output with different GCM forcing's
 180 wereutilized to develop multi-model ensemble projections employing Bayesian model averaging
 181 (BMA)technique. BMA is an advanced statistical technique for deriving the multi-model
 182 ensemble and combines the individual models using optimized weights; weights being
 183 proportional to the relative skills of models in reproducing observed data.The regression model
 184 in BMA takes into account all conceivable combinations of variables (in this case, GCMs) before
 185 calculating a weighted average. The Posterior Model Probability (PMP) used as weight, is a
 186 measure of model's skillduring training(Raftery et al., 2005). Suppose we have k models; the
 187 maximum count of regression models is $s = 2^k$. Here in the study using 6models, the number of
 188 regression models is $s = 2^6 = 64$. PMP of n -th model $P(M_n | D)$,in 2^k candidate regression models
 189 is computed using Bayes theorem as given in Eq.4

$$P(M_n | D) = \frac{p(D | M_n) \cdot p(M_n)}{p(D)} \quad (4)$$

190

191

192 Where $p(D | M_n)$ is the observed data likelihood given n -thmodel, $p(M_n)$ is the n -th regression
 193 model's prior probability and $p(D)$ is a constant used for normalizing as given in Eq.5,

$$p(D) = \sum_{n=1}^s p(D | M_n) \cdot p(M_n) \quad (5)$$

194 Different forms of priors are available in the literature, and for this investigation, we selected a
 195 uniform prior distribution based on Khan et al., (2021), which gives equal weight to all possible
 196 regression models. For the likelihood function $p(D | M_n)$, Gaussian likelihood (Vogel et al.,
 197 2008) was used following Khan et al., (2021). Eq.6 gives the variable's conditional prediction
 198 PDF based on training data.

$$p(y | D) = \sum_{n=1}^s p(y | M_n, D) \cdot p(M_n | D) \quad (6)$$

199

200

201 Where $p(y | M_n)$ is the prediction PDF based on n -th regression model and $p(M_n | D)$ is the
 202 associated posterior probability and is being used as weight (Khan et al., 2021).

203 3.5 SWAT Model setup

204 Hydrological modeling is a key aspect in evaluating the hydrological implications of climatic
 205 changes (Praskievicz & Chang, 2009). The basin was modelled by employing the SWAT
 206 hydrological model to project the changes in streamflow and water budget components for the
 207 21st century. The water balance in the model is governed by Eq.7 given below:

$$SW_t = SW_0 + \sum_{i=1}^n (R_{day} - Q_{surf} - E_a - w_{seep} - Q_{gw}) \quad (7)$$

208 Where SW_t denotes the water content of soil at t timestep, SW_0 denotes the initial water content of
 209 soil, R_{day} is daily precipitation, Q_{surf} denotes the surface runoff, E_a denotes the
 210 Evapotranspiration, w_{seep} denotes the percolation and Q_{gw} denotes the groundwater
 211 flow (Bajracharya et al., 2018). The units of all components are in millimeters (mm).

212 Snowmelt was incorporated in the runoff calculations and is governed by the Eq. 8,

$$SNOW_{melt} = b_{melt} * snowcov \left(\left(\frac{T_{snow} + T_{max}}{2} \right) - T_{melt} \right) \quad (8)$$

213 where, $SNOW_{melt}$ denotes the amount of daily snowmelt (mm), b_{melt} denotes the factor of daily
 214 melt (mm/day °C), $snowcov$ denotes the fraction of snow-cover in HRU area, T_{max} is the day's
 215 maximum temperature., T_{snow} is the temperature of snowpack (°C) and T_{melt} denotes the snowmelt
 216 threshold temperature (°C) (Bhatta et al., 2019).

217 SWAT uses various inputs viz., climate data, soil map/attributes, land use map/attributes, Digital
 218 Elevation Model (DEM), and the observed streamflow. The weather database for the calibrating
 219 and validating SWAT model was prepared using the observed meteorological data for
 220 Temperature (T_{max} , T_{min}) and Precipitation variables while for Solar Radiation, Wind Speed,
 221 and Relative Humidity, CFSR dataset was collated. For the elevation inputs, ALOS PALSAR
 222 DEM having a grid size of 12.5m was used (<https://search.asf.alaska.edu/#/>). The land use/land
 223 cover data for the region was produced by the supervised classification of Landsat 8 OLI
 224 imagery acquired on 2013/06/03, in ArcGIS 10.2. The soil layer and the associated attributes for
 225 the study area were accessed through the SWAT website under India datasets
 226 (<https://swat.tamu.edu/data/india-dataset/>).

227 DEM was employed as an input in the *qswat* interface of the SWAT model to divide the
 228 catchment into sub-basins. A threshold of 10000 ha was used in the delineation of the drainage
 229 network and the analysis identified 41 sub-basins in the Jhelum basin. The smallest model unit is
 230 the Hydrological Response Unit (HRU), which is defined by a unique fusion of soil type, slope
 231 class, and land use. (Romagnoli et al., 2017). Since the seasonal snowmelt determines the basin's
 232 hydrology, elevation bands were created to represent the snowmelt as well as the orographic
 233 controls of precipitation and temperature. SWAT model provides a maximum of 10 elevation
 234 bands for a particular sub-basin and in the present analysis 5 elevation bands were set for the
 235 sub-basins having a significant altitudinal range whereas for sub-basins with less orographic
 236 differences only one elevation band was used e.g., Bajracharya et al., (2018).

237 3.6 SWAT model calibration and validation

238 Multi-site calibration and validation were carried for the 3 gauges on the trunk stream viz.,
 239 Sangam, Asham, and Ram Munshi Bagh. Observed monthly streamflow data for 10 yrs (2002-

240 2011) were used in calibration while as 5yrs (2012-2016) were used in the validation of the
241 model. Before the calibration of the model, sensitivity analysis was carried to filter the most
242 influential parameters determining the streamflow variations. The parameters were ranked as per
243 their sensitivity towards the streamflow using the global sensitivity analysis embedded in the
244 SUFI-2. It employs the p-stat and t-stat to determine the most sensitive parameters, having lower
245 p-values and higher t-values (Bhatta et al., 2019). The SWAT-CUP considers the parameter
246 uncertainty, model uncertainty, input error, and yields uncertainty measures like 95% prediction
247 uncertainty (95PPU), r-factor and p-factor. The p-factor refers to percentage of the observed data
248 series that is encompassed by the 95PPU, and ranges between 0 to 1. Similarly, the r-factor,
249 which runs from 0 to 1, is the mean width of the 95PPU divided with the standard deviation of
250 the observational datasets. The higher p-factor values (towards 1) and lower r-factor values
251 (towards 0) imply the better simulation of the hydrology and thus stream flows (Uniyal et al.,
252 2015). Statistical indicators such as R^2 , PBIAS, and NSE were also utilized to assess model
253 performance. Moriasi et al., (2007) and Almeida et al., (2018) have defined the thresholds of
254 satisfactory and acceptable model performance for $0.50 < R^2 \leq 0.60$, $\pm 15 < \text{PBIAS} \leq \pm 25$, and
255 $0.36 < \text{NSE} \leq 0.60$.

256 Multi-model ensemble climatic projections were coupled with the calibrated and
257 validated model to simulate the hydrological implications of changing climatic patterns in the
258 Jhelum basin. After ascertaining the robustness of BMA projections, these were utilized as an
259 input to project the streamflow at Ram Munshi Bagh, Asham, and Sangam gauges under RCP4.5
260 and RCP8.5. Moreover, the impact of climatic changes was assessed separately on the different
261 components of catchment water balance viz., evapotranspiration, snowmelt, surface runoff, and
262 water yield. Due to paucity of observed data, the SWAT simulated output for these components
263 during the baseline run (2001-2010) was used as reference to estimate the relative changes over
264 the 21st century (Bajracharya et al., 2018).

265 **4. Results**

266 *4.1 Bias -correction of the GCM/RCM output*

267 The competence of the bias correction techniques was evaluated by the comparison RCM data
268 (raw & BC) with the observational data on a monthly scale, using efficiency metrics viz., R^2 ,

269 PBIAS, and NSE (Table 2). For Tmax and Tmin, R² values were high before bias correction but
270 PBIAS and NSE got significantly improved. The raw Tmax (Tmin) displayed substantial biases
271 and bias correction minimized the PBIAS from -60.6 – -37.40 (-135 – -47.2) to 1.9 – 3.9 (2.3 –
272 6.5). Likewise, the NSE values for Tmax (Tmin) in raw RCM were of the order -0.84 – 0.06 (-
273 0.29 – 0.55) and bias correction improved the values to 0.89 – 0.91 (0.92 – 0.95). In contrast to
274 this, GCMs tend to resolve the precipitation poorly as indicated by lower values of efficiency
275 metrics. However, the bias correction could improve the match among the simulated and the
276 observational data (Table 2). Furthermore, Taylor Diagrams (Taylor, 2001) are used to display
277 the RCM's performance (raw and BC) (Fig 2).

278 Considering the uncertainty in the single RCM output, multi-model ensemble projections were
279 derived using BMA and were also compared with the baseline data. The BMA ensemble data
280 matched closely with the observed data than any of the individual RCMs, supported by the
281 increased values of the efficiency indicators (Table 2). The PBIAS in the BMA estimates of
282 climatic variables reduced to 0 along with further improvements in R² and NSE. Fig 3 depicts the
283 performance of the BMA technique during the training period.

284 *4.2 Climate change projections for 21st century*

285 The projections from the individual models and the BMA ensemble for the Jhelum basin are
286 presented in Table 3. The results infer substantial warming in the annual mean maximum (Tmax)
287 and minimum (Tmin) temperatures with varying rates of warming among the different GCMs.
288 Multi-model ensemble projections show that under RCP4.5 the Tmax (Tmin) of the region will
289 increase by 0.41 (1.39) °C during 2020s, 1.80 (2.12) °C during 2050s, and 2.31 (2.37) °C during
290 2080s. The rate of the warming for Tmax (Tmin) enhances under the RCP8.5 forcing levels by
291 increments of 0.63 (2.14) °C during 2020s, 2.56 (3.12) °C during 2050s, and 4.82 (4.35)
292 °C during 2080s. While comparing the magnitude of changes simulated by the different models, it
293 varied substantially e.g., for Tmax, it varied from 0.81°C (CNRM-CM5) to 1.42°C (MPI-ESM-
294 MR) for the 2020s, 1.59°C (CNRM-CM5) to 3.01°C (CSIRO-Mk3) for 2050s, and 2.17°C
295 (CNRM-CM5) to 3.66°C (CSIRO-Mk3) for 2080s under RCP4.5 forcing levels. CNRM -CM5
296 shown consistently least amount of the change for Tmax and Tmin during the different spans of
297 the 21st century under both RCPs. The station scale BMA projections (Table 4) reveal higher
298 warming rates in Tmax and Tmin for the Gulmarg while the lowest warming rates were found

299 for Srinagar (Tmax) and Pahalgam (Tmin). Moreover, ensemble estimates project enhanced night-
300 time warming in the region over the 21st century pinpointed by the higher warming rates of
301 Tmin as compared to the Tmax. The asymmetrical warming patterns of Tmax and Tmin exist
302 even between models and also among the different spans of the 21st century e.g., the CSIRO-
303 Mk3 model projects higher rates of warming in Tmin than Tmax for the 2020s and vice versa
304 during the 2050s and 2080s. The BMA projections for the Tmax and Tmin in the Jhelum basin
305 are shown graphically in Fig 4a and Fig 4b respectively.

306 Precipitation projections for the Jhelum basin show reduction over the 21st century vis-a-vis the
307 baseline (1980-2010). The BMA estimates project decreases of order 7.2- 4.57 % (RCP4.5) and
308 4.75-2.47 % (RCP8.5) during the different periods of the 21st century. Despite the fact that
309 precipitation tends to increase from the 2020s to the 2080s (Fig 4c), there is a net decrease when
310 compared to baseline values. The diminishing patterns of precipitation rhyme across all
311 the individual models although with higher magnitudes than BMA estimates (Table 3), except
312 IPSL-CM5A-LR which projects an increase of 9.6 % in the precipitation of the Jhelum basin
313 during the 2080s under RCP8.5. The station scale BMA estimates (Table 4) show enhanced
314 decreases for Kokernag (RCP4.5 and 8.5), Kupwara (RCP4.5 and 8.5), and Gulmarg (RCP8.5). In
315 contrast to this, stations like Gulmarg (RCP4.5), and Qazigund (RCP 8.5) witness increases in
316 the precipitation while the Srinagar shows almost no change (< 1%) over the 21st century when
317 compared with the baseline precipitation.

318 *4.3 SWAT model calibration and validation*

319 Any hydrological model must be adequately calibrated and validated before adopting its outputs
320 for further analysis. The SUFI-2 algorithm, embedded within the SWAT-CUP was employed to
321 calibrate and validate SWAT. Multi-site calibration was done for Sangam, Asham, and Ram
322 Munshi Bagh gauges, located on the trunk stream using the observed mean monthly streamflow
323 values for 2000-2010. The model was validated using 5yr (2011-2016) streamflow data. Prior to
324 that, sensitivity analysis was executed to limit the count of parameters. Table 5 shows the 11 most
325 sensitive parameters as well as their p-value and t-stat, important in the estimation of streamflow
326 variability. The model conformity during its calibrating and validating process was assessed using
327 3 statistical indicators viz., R², PBIAS, and NSE. Furthermore, uncertainty of the model outputs
328 was evaluated using the r-factor and p-factor. Table 6 shows the performance metrics of the

329 SWAT model and the values reflect that model performance was well within the acceptable
330 limits. The close agreement between actual and modelled streamflow (Fig 5) reveals that the
331 validated model could be employed with considerable confidence and accuracy to model
332 hydrologic responses to climatic changes.

333 *4.5 Projection of streamflow's under climate change scenario's*

334 After the calibration and validation, SWAT was employed to translate the climatic change signals
335 into streamflow responses using the multi-model ensemble climatic projections obtained using
336 BMA. The relative changes in the streamflow during the different spans of 21st century was
337 compared with the baseline (2001-2010) values for 3 gauges (Sangam, Asham, and Ram
338 Munshi Bagh) located along the course of the trunk stream (Table 7). In the wake of rising
339 temperatures and declining precipitation patterns, the Jhelum basin is going to witness
340 substantial reductions in streamflow over the 21st century. Under RCP4.5 forcing levels, the
341 decreases are of the order 23-27% during 2020s, 30-35% during 2050s, and 31-37% during
342 2080s. With intensifications in the radiative forcing level under RCP8.5, the reductions also get
343 enhanced with magnitudes of 19-25% during 2020s, 31-37% during 2050s, and 40-46%
344 during 2080s. In comparison to the baseline values, seasonal streamflow tended to decline over
345 time. Summer (JJA) witnesses most of the decreases followed by Winter (DJF) and Spring
346 (MAM) under both RCPs. Summer shows a maximum reduction during the 2080s, by about 46-
347 52% under RCP4.5 and 61-67% under RCP8.5. Moreover, Autumn (SON) is the least affected
348 and shows only minimal changes in streamflow's over the 21st century. For illustrative purposes,
349 the projected variations in mean monthly, annual and, seasonal streamflow's of river Jhelum at
350 Asham gauge under both the RCPs are shown in Fig 6.

351 *4.6 Projection of water budget components under climatic change scenario's*

352 The variations in the streamflow are governed and linked with the different components of water
353 balance like precipitation, evapotranspiration, surface runoff, snowmelt, etc. After having the
354 precipitation projections for the 21st century, the current study also intended to assess the relative
355 changes in other water balance components viz., Actual Evapotranspiration (ET), Potential
356 Evapotranspiration (PET), Snowmelt, Surface runoff (SurQ), and Water yield (Wyield) under
357 climate change scenarios. These components were simulated using the SWAT model for the

358 baseline period (2001-2010) from the observational climate data and BMA ensemble climatic
359 projections were employed for the future simulations. Due to lack of observed data, the SWAT
360 simulated output for these components during the baseline run (2001-2010) was used as
361 reference data(Bajracharya et al., 2018). The percentage changes in the water budget components
362 throughout various time periods in the 21st century, under both RCPs were calculated by
363 comparing them to baseline values. Fig 7 shows the projected changes in the Jhelum basin's
364 average annual hydrological components over different time periods in the future.

365

366 ET was estimated from the Hargreaves method (Hargreaves and Samani, 1985), and it witnessed
367 increases over the 21st century in the Jhelum basin. Actual ET shows increases of order 18 (20)
368 during 2020s, 28(30) during 2050s, and 31(40) % during 2080s under RCP4.5 (RCP8.5). The
369 changes in the ET for different sub-basins over 21st century under both RCPs is shown in Fig 8.
370 ET projections show a progressive increase for the future, determined by levels of radiative
371 forcing and time viz., near, mid or end century. This increase in the ET aligns with the projected
372 increase in the temperatures driven by the enhanced radiative forcing levels. Due to the
373 continuously rising temperatures, the ET values show a consistent rise over the 21st century. ET
374 constitutes a major abstraction in the water balance which reduces the net water availability for
375 the runoff and is a measure of the irrigation water requirements.

376 Snowmelt contribution in the Jhelum basin witnessed significant decreases in future under the
377 changing climatic regimes. The snowmelt shows substantial reductions by about 53(50) %
378 during 2020s, 58(62) % during 2050s, and 60(72) % during 2080s under RCP4.5 (RCP8.5).
379 Moreover, Fig 9 reveals that most of the decreases will be observed in the sub-basins situated in
380 the lower elevation. The decrease in Snowmelt contribution may be attributed to the declining
381 precipitation trends over the 21st century. Jhelum basin is projected to witness decreases in the
382 overall precipitation, and this would mean a reduction in the winter season precipitation too that
383 is in the form of snowfall. Significant decreasing trends are already ominous in the winter season
384 precipitation of the Jhelum basin (Ahsan et al., 2021a). Furthermore, the warming temperatures
385 would also reduce the precipitation amount falling as snow and there will be more liquid
386 precipitation.

387 Water yield is a measure of the cumulative water delivered to streamflow by sub-basins/HRUs,
388 and includes baseflow, lateral flow, and surface runoff (Andrade et al., 2021; Jain et al.,
389 2017).The average water yieldwithin the Jhelum basinwitnessed a decline over 21st century. For
390 the RCP4.5 (RCP8.5), the water yield witnesses' reductions by 17.7(18.4) % during 2020s, 24
391 (32) % during 2050s, and 25 (42) % during 2080s. Fig 10 shows the spatial variations in the
392 projected water yield of different sub-basins for different spans of the future. The projected
393 decreases in the water yield can be attributed to the enhancement of the ET levels and decreases
394 in the snowmelt contribution over the 21st century.The progressive decline in the water yield
395 during the 21st century infers that water availability will get reduced significantly and will
396 aggravate the water scarcity and stresses in the basin.

397 **5. Discussions**

398 The water resources of the mountainous basins are highly exposed to climatic changes wherein
399 the regional hydrology is dependent on the glacial ice melt and seasonal snowmelt
400 characteristics. The present study is attempted in the Jhelum basin- nestled in the complex folds
401 of North-Western Himalayas and forms important headwaters ofthe Indus River system. The
402 imprints of global climate change are well established from the observational datasets in the
403 Jhelum basin and its impacts are already being felt(Ahsan et al., 2021a). Few studies e.g., (Ahsan
404 et al., 2021b) have also attempted to estimate the magnitude of climatic changes over the 21st
405 century. However, these studies are limited in scope because the projections are based on a
406 single GCM.It has been found that GCM outputs inherit considerable uncertainty in them and
407 thus use of a single GCM can yield inaccurate results(Khan et al., 2021). For modeling the
408 hydrological consequences of climatic changes, the development of rigorous and robust climate
409 change projections is a primary requirement. To this end,6 GCMs dynamically downscaled by
410 the RegCM4 RCM from the CORDEX-SA experiments under a medium stabilizing forcing level
411 (RCP4.5) and an extreme forcing level (RCP8.5), were collated for the present study. The use of
412 RCM output is preferred for the basin-scale assessment than the GCM due to their higher
413 resolution and the local sub-grid processesare parametrized better(Seager&Vecchi, 2010).
414 However, the raw RCM outputs may still contain significant biases particularly over
415 mountainousareas(Fowler et al., 2007).As a result, bias correcting the RCM ouputs is critical,
416 and in this work, temperature was bias-corrected using the VS approach, and precipitation was

417 bias-corrected using a mix of LOCI and PT techniques. The bias correction significantly
418 improved the performance indicators and yielded an overall better match between the
419 observational data and the RCM simulation results during the baseline (1980-2010). Furthermore,
420 to narrow the uncertainty, multi-model ensemble climate change projections were developed
421 using the Bayesian Model Averaging (BMA) technique. There is consensus among the climate
422 modeling community that by using the multi-model ensemble climatic projections, the
423 uncertainty can significantly reduce, given the fact that individual models may simulate different
424 aspects of the climate system well and the errors get canceled or reduced in the process (Brient,
425 2019). Moreover, it has been reported that by using the multiple simulations from a given RCM
426 for different GCM forcings and emission scenarios, accuracy of climatic projections can be further
427 improved (Raisanen et al., 2004; van den Hurk et al., 2005; Salathe, 2005).

428 The climate change projections from all the GCMs and BMA estimates show
429 unequivocal warming for the Jhelum basin over 21st century. The increments in temperature are
430 progressive over time and varies directly with levels of radiative forcing levels. BMA
431 estimates project warming of Tmax by 0.41-2.37 (0.63-4.82) during the various spans of the
432 future under RCP4.5(RCP8.5). Tmin is getting warmer at a relatively higher rate vis-a-
433 vis Tmax and increases are of the order 1.39-2.37 °C under RCP4.5 and 2.14-4.35 °C under RCP8.5.
434 Precipitation in the Jhelum basin witnessed reductions by varying amounts across different
435 GCMs. These changing climatic regimes are going to trigger several implications for key sectors
436 viz., water resources, agriculture, energy consumption, or human health (Ahsan et al., 2021a).
437 The possible implications on the streamflow and water budget of the basin were assessed by
438 coupling the climate change scenarios into the SWAT model. SWAT model performed quite
439 well in simulating the basin hydrology as inferred by high values of the model skill metrics. The
440 streamflow of the river Jhelum is projected to witness substantial reductions over the 21st century
441 under both RCP's. The decreases aggravate over time and forcing levels with the highest
442 decrease of about 40-46% for the 2080s under RCP8.5. These reductions in streamflow are driven
443 by influences of climatic changes on the different components of water budget like
444 Evapotranspiration and snowmelt. Both potential and actual ET are showing a rise over 21st
445 century in response to the projected warming. Actual ET in the Jhelum basin witnessed
446 a maximum increase of 31% under RCP4.5 and 40% under RCP8.5 during 2080s. Increases in the
447 ET under climatic warming has been stated in other relevant studies like Andrade et al.,

448 (2021), Bajracharya et al., (2018) and Reshmidevi et al., (2018). Snowmelt is another important
449 component of regional hydrology and sustains the streamflows in Jhelum basin during the dry
450 months (Jeelani et al., 2012). Under the changing climate, snowmelt witness a reduction of 50-
451 70% over the 21st century. The decrease in the snowmelt may be attributed to the coupled impact
452 of warming temperatures and diminishing precipitation. Higher temperatures particularly during
453 the winter would cause more precipitation in the form of rain than snow and would ultimately
454 decrease the snowmelt contributions. The decreasing snow and increasing rain proportion in the
455 precipitation are already being observed in the basin as reported by Romshoo et al., (2018). This
456 will also lead to the enhanced ablation of the glacial reserves in the basin. The glacial recession
457 has amplified significantly in the region during the last few decades (Murtaza & Romshoo,
458 2016). Another important aspect of the snowmelt characteristic driven by the increasing
459 temperatures is the earlier melting of the snowpacks. This impact is discernible during the 2080s
460 under RCP8.5 where the peak streamflow month is showing a shift from May to March (Fig
461 6c). This shifting of peak streamflow has been reported in the numerous other snow-fed basins of
462 the world and tends to create issues for water resource management due to shifting of peak
463 streamflow period away from peak demand season (Barnett et al., 2005). The combined impacts
464 of the ET and snowmelt are yielding a decrease in water yield of the basin and hence
465 streamflow's.

466 **6. Conclusions**

467 The discharge from the rivers in the Jhelum basin is of tremendous importance from the
468 perspective of ecology, environmental health, and water security. The river waters are generally
469 tapped for irrigation, hydropower generation, domestic consumption, and recreation purposes.
470 Hence, any changes in hydrological conditions induced by the climatic changes will entail a
471 profound influence on the environment and the society. With the application of multiple
472 downscaled GCMs, the present study projects the magnitude of climatic changes and its
473 hydrological repercussions in the Jhelum basin for the 21st century. The changes are projected for
474 the annual mean maximum and minimum temperatures, precipitation percentages and river
475 discharge. This analysis found that the maximum temperature may rise up to 4.82°C and
476 minimum temperature may go up by 4.35°C coupled with reduction in the precipitation to the
477 maximum of 7.2% in the given time period. Consequent to the changes in temperature and
478 precipitation conditions, the discharge of the rivers is likely to fall by 17 to 42%. The increase in

479 temperature, decline in the precipitation, and the huge decrease in the seasonal flow of rivers
480 may result in dwindling aquatic ecosystems, loss of biodiversity, reduced productivity, and
481 conflicts in water sharing agreements e.g., Indus Water Treaty. The deliverables of the study may
482 therefore serve as a guide for foreseeing the future challenges and developing policies to mitigate
483 and adapt to the changing climate and the flow regimes of the river basins in the Himalaya.

484 **Acknowledgements**

485 The Working Group on Regional Climate of the World Climate Research Programme, as well as
486 the Working Group on Coupled Modelling, which served as CORDEX's former
487 coordinating body and was responsible for CMIP5, are respectfully recognized. The authors are
488 grateful to the climate modelling groups for creating and making their model results public.
489 CORDEX South Asia data was provided via the Earth System Grid Federation (ESGF)
490 infrastructure and the Climate Data Portal at the Indian Institute of Tropical Meteorology (IITM)
491 for Climate Change Research (CCCR).

492 **Funding**

493 This research has been funded by University Grants Commission, New Delhi, under CPEPA
494 scheme being currently carried out at University of Kashmir, Srinagar-190006.

495
496
497
498
499
500
501
502
503
504
505
506
507
508
509
510
511
512
513
514
515
516
517
518
519

520
521
522
523
524
525
526
527
528
529

References

- 530 Abbaspour, K. C., Yang, J., Maximov, I., Siber, R., Bogner, K., Mieleitner, J., Zobrist, J., &
531 Srinivasan, R. (2007). Modelling hydrology and water quality in the pre-alpine/alpine Thur
532 watershed using SWAT. *Journal of Hydrology*, 333(2–4), 413–430.
533 <https://doi.org/10.1016/J.JHYDROL.2006.09.014>
- 534 Ahsan, S., Bhat, M. S., Alam, A., Ahmed, N., Farooq, H., & Ahmad, B. (2021a). Assessment of
535 trends in climatic extremes from observational data in the Kashmir basin, NW Himalaya.
536 *Environmental Monitoring and Assessment*, 193(10). [https://doi.org/10.1007/S10661-021-09439-](https://doi.org/10.1007/S10661-021-09439-7)
537 7
- 538 Ahsan, S., Bhat, M. S., Alam, A., Farooq, H., & Shiekh, H. A. (2021b). Evaluating the impact of
539 climate change on extreme temperature and precipitation events over the Kashmir Himalaya.
540 *Climate Dynamics*, 1, 1–19. <https://doi.org/10.1007/S00382-021-05984-6/FIGURES/7>
- 541 Alam, A., Ahmad, S., Bhat, M. S., & Ahmad, B. (2015). Tectonic evolution of Kashmir basin in
542 northwest Himalayas. *Geomorphology*, 239, 114–126.
543 <https://doi.org/10.1016/j.geomorph.2015.03.025>
- 544 Alam, A., Bhat, M. S., Kotlia, B. S., Ahmad, B., Ahmad, S., Taloor, A. K., & Ahmad, H. F.
545 (2017). Coexistent pre-existing extensional and subsequent compressional tectonic deformation
546 in the Kashmir basin, NW Himalaya. *Quaternary International*, 444(Part A), 201–208.
547 <https://doi.org/10.1016/j.quaint.2017.06.009>
- 548 Alam, A., Bhat, M. S., & Maheen, M. (2020). Using Landsat satellite data for assessing the land
549 use and land cover change in Kashmir valley. *GeoJournal*, 85(6), 1529–1543.
550 <https://doi.org/10.1007/S10708-019-10037-X/TABLES/4>
- 551 Almeida, R. A., Pereira, S. B., & Pinto, D. B. F. (2018). Calibration and validation of the SWAT
552 hydrological model for the Mucuri river basin. *Engenharia Agricola*, 38(1), 55–63.
553 <https://doi.org/10.1590/1809-4430-ENG.AGRIC.V38N1P55-63/2018>
- 554 Andrade, C. W. L., Montenegro, S. M. G. L., Montenegro, A. A. A., Lima, J. R. de S.,
555 Srinivasan, R., & Jones, C. A. (2021). Climate change impact assessment on water resources

556 under RCP scenarios: A case study in Mundaú River Basin, Northeastern Brazil. *International*
557 *Journal of Climatology*, 41(S1), E1045–E1061. <https://doi.org/10.1002/joc.6751>

558 Bajracharya, A. R., Bajracharya, S. R., Shrestha, A. B., & Maharjan, S. B. (2018). Climate
559 change impact assessment on the hydrological regime of the Kaligandaki Basin, Nepal. *Science*
560 *of the Total Environment*, 625, 837–848. <https://doi.org/10.1016/j.scitotenv.2017.12.332>

561 Barnett, T. P., Adam, J. C., & Lettenmaier, D. P. (2005). Potential impacts of a warming climate
562 on water availability in snow-dominated regions. *Nature*, 438(7066), 303–309.
563 <https://doi.org/10.1038/NATURE04141>

564 Bhat, M. S., Alam, A., Ahmad, B., Kotlia, B. S., Farooq, H., Taloor, A. K., & Ahmad, S. (2018).
565 Flood frequency analysis of river Jhelum in Kashmir. *Quaternary International*, 507, 288–294.
566 <https://doi.org/10.1016/j.quaint.2018.09.039>

567 Bhatta, B., Shrestha, S., Shrestha, P. K., & Talchabhadel, R. (2019). Evaluation and application
568 of a SWAT model to assess the climate change impact on the hydrology of the Himalayan River
569 Basin. *CATENA*, 181, 104082. <https://doi.org/10.1016/J.CATENA.2019.104082>

570 Brient, F. (2019). Reducing Uncertainties in Climate Projections with Emergent Constraints:
571 Concepts, Examples and Prospects. *Advances in Atmospheric Sciences* 2020 37:1, 37(1), 1–15.
572 <https://doi.org/10.1007/S00376-019-9140-8>

573 Chen, J., Brissette, F. P., Chaumont, D., & Braun, M. (2013). Performance and uncertainty
574 evaluation of empirical downscaling methods in quantifying the climate change impacts on
575 hydrology over two North American river basins. *Journal of Hydrology*, 479, 200–214.
576 <https://doi.org/10.1016/J.JHYDROL.2012.11.062>

577 de Oliveira, V. A., de Mello, C. R., Viola, M. R., & Srinivasan, R. (2017). Assessment of climate
578 change impacts on streamflow and hydropower potential in the headwater region of the Grande
579 river basin, Southeastern Brazil. *International Journal of Climatology*, 37(15), 5005–5023.
580 <https://doi.org/10.1002/joc.5138>

581 Dimri, A. P., Kumar, D., Choudhary, A., & Maharana, P. (2018). Future changes over the
582 Himalayas: Mean temperature. *Global and Planetary Change*, 162, 235–251.
583 <https://doi.org/10.1016/J.GLOPLACHA.2018.01.014>

584 Fang, G. H., Yang, J., Chen, Y. N., & Zammit, C. (2015). Comparing bias correction methods in
585 downscaling meteorological variables for a hydrologic impact study in an arid area in China.
586 *Hydrology and Earth System Sciences*, 19(6), 2547–2559. [https://doi.org/10.5194/HESS-19-](https://doi.org/10.5194/HESS-19-2547-2015)
587 2547-2015

588 Fowler, H. J., Ekström, M., Blenkinsop, S., & Smith, A. P. (2007). Estimating change in extreme
589 European precipitation using a multimodel ensemble. *Journal of Geophysical Research:*
590 *Atmospheres*, 112(D18). <https://doi.org/10.1029/2007JD008619>

591 Giorgi, F., Coppola, E., Solmon, F., Mariotti, L., Sylla, M. B., Bi, X., Elguindi, N., Diro, G. T.,
592 Nair, V., Giuliani, G., Turuncoglu, U. U., Cozzini, S., Güttler, I., O'Brien, T. A., Tawfik, A. B.,
593 Shalaby, A., Zakey, A. S., Steiner, A. L., Stordal, F., ... Brankovic, C. (2012). RegCM4: model
594 description and preliminary tests over multiple CORDEX domains. *Climate Research*, 52(1), 7–
595 29. <https://doi.org/10.3354/CR01018>

596 Gleckler, P. J., Taylor, K. E., & Doutriaux, C. (2008). Performance metrics for climate models.
597 *Journal of Geophysical Research: Atmospheres*, 113(D6).
598 <https://doi.org/10.1029/2007JD008972>

599 Hao, Y., Ma, J., Chen, J., Wang, D., Wang, Y., & Xu, H. (2018). Assessment of changes in water
600 balance components under 1.5 °C and 2.0 °C global warming in transitional climate basin by
601 multi-RCPs and multi-GCMs approach. *Water (Switzerland)*, 10(12).
602 <https://doi.org/10.3390/w10121863>

603 Hargreaves, G. H., & Samani, Z. A. (1985). Reference crop evapotranspiration from
604 temperature. *Applied engineering in agriculture*, 1(2), 96-99.

605 Huang, Y. (2014). Comparison of general circulation model outputs and ensemble assessment of
606 climate change using a Bayesian approach. *Global and Planetary Change*, 122, 362–370.
607 <https://doi.org/10.1016/J.GLOPLACHA.2014.10.003>

608 Huntington, T. G. (2006). Evidence for intensification of the global water cycle: Review and
609 synthesis. *Journal of Hydrology*, 319(1–4), 83–95.
610 <https://doi.org/10.1016/J.JHYDROL.2005.07.003>

611 Immerzeel, W. W., Pellicciotti, F., & Bierkens, M. F. P. (2013). Rising river flows throughout the
612 twenty-first century in two Himalayan glacierized watersheds. *Nature Geoscience*, 6(9), 742–
613 745. <https://doi.org/10.1038/NGEO1896>

614 Jain, S., Jain, S., Jain, N., & Xu, C.-Y. (2017). Hydrologic modeling of a Himalayan mountain
615 basin by using the SWAT mode. *Hydrology and Earth System Sciences Discussions*, 1–26.
616 <https://doi.org/10.5194/HESS-2017-100>

617 Jasper, K., Calanca, P., Gyalistras, D., & Fuhrer, J. (2004). Differential impacts of climate
618 change on the hydrology of two alpine river basins. *Climate Research*, 26(2), 113–129.
619 <https://doi.org/10.3354/CR026113>

620 Jeelani, G., Feddema, J. J., van der Veen, C. J., & Stearns, L. (2012). Role of snow and glacier
621 melt in controlling river hydrology in Liddar watershed (western Himalaya) under current and
622 future climate. *Water Resources Research*, 48(12). <https://doi.org/10.1029/2011WR011590>

623 Khan, F., Pilz, J., & Ali, S. (2021). Evaluation of CMIP5 models and ensemble climate
624 projections using a Bayesian approach: a case study of the Upper Indus Basin, Pakistan.
625 *Environmental and Ecological Statistics*, 28(2), 383–404. <https://doi.org/10.1007/s10651-021-00490-8>

627 Knutti, R., Furrer, R., Tebaldi, C., Cermak, J., & Meehl, G. A. (2010). Challenges in Combining
628 Projections from Multiple Climate Models. *Journal of Climate*, 23(10), 2739–2758.
629 <https://doi.org/10.1175/2009JCLI3361.1>

630 Krishnan, R., Shrestha, A. B., Ren, G., Rajbhandari, R., Saeed, S., Sanjay, J., Syed, Md. A.,
631 Vellore, R., Xu, Y., You, Q., & Ren, Y. (2019). Unravelling Climate Change in the Hindu Kush
632 Himalaya: Rapid Warming in the Mountains and Increasing Extremes. *The Hindu Kush*
633 *Himalaya Assessment*, 57–97. https://doi.org/10.1007/978-3-319-92288-1_3

634 Krysanova, V., & Hattermann, F. F. (2017). Intercomparison of climate change impacts in 12
635 large river basins: overview of methods and summary of results. *Climatic Change*, 141(3), 363–
636 379. <https://doi.org/10.1007/S10584-017-1919-Y/TABLES/5>

637 Kundzewicz, Z. W., Mata, L. J., Arnell, N. W., DÖLL, P., Jimenez, B., Miller, K., Oki, T., ŞEN,
638 Z., & Shiklomanov, I. (2008). The implications of projected climate change for freshwater
639 resources and their management. *Hydrological Sciences Journal*, 53(1), 3–10.
640 <https://doi.org/10.1623/HYSJ.53.1.3>

641 Liu, L., Liu, Z., Ren, X., Fischer, T., & Xu, Y. (2011). Hydrological impacts of climate change
642 in the Yellow River Basin for the 21st century using hydrological model and statistical
643 downscaling model. *Quaternary International*, 244(2), 211–220.
644 <https://doi.org/10.1016/j.quaint.2010.12.001>

645 Lone, S. A., Jeelani, G., Alam, A., Bhat, M. S., & Farooq, H. (2021) Effect of Changing Climate
646 on the Water Resources of Upper Jhelum Basin (UJB), India.

647 Luo, M., Liu, T., Meng, F., Duan, Y., Bao, A., Xing, W., Feng, X., de Maeyer, P., & Frankl, A.
648 (2019). Identifying climate change impacts on water resources in Xinjiang, China. *Science of The*
649 *Total Environment*, 676, 613–626. <https://doi.org/10.1016/J.SCITOTENV.2019.04.297>

650 Lutz, A. F., Immerzeel, W. W., Shrestha, A. B., & Bierkens, M. F. P. (2014). Consistent increase
651 in High Asia’s runoff due to increasing glacier melt and precipitation. *Nature Climate Change*,
652 4(7), 587–592. <https://doi.org/10.1038/NCLIMATE2237>

653 Massoud, E. C., Lee, H., Gibson, P. B., Loikith, P., & Waliser, D. E. (2020). Bayesian Model
654 Averaging of Climate Model Projections Constrained by Precipitation Observations over the
655 Contiguous United States. *Journal of Hydrometeorology*, 21(10), 2401–2418.
656 <https://doi.org/10.1175/JHM-D-19-0258.1>

657 Meinshausen, M., Smith, S. J., Calvin, K., Daniel, J. S., Kainuma, M. L. T., Lamarque, J.,
658 Matsumoto, K., Montzka, S. A., Raper, S. C. B., Riahi, K., Thomson, A., Velders, G. J. M., &
659 van Vuuren, D. P. P. (2011). The RCP greenhouse gas concentrations and their extensions from
660 1765 to 2300. *Climatic Change*, 109(1), 213–241. [https://doi.org/10.1007/S10584-011-0156-
Z/TABLES/5](https://doi.org/10.1007/S10584-011-0156-
661 Z/TABLES/5)

662 Moriasi, D. N., Arnold, J. G., Liew, M. W. van, Bingner, R. L., Harmel, R. D., & Veith, T. L.
663 (2007). Model Evaluation Guidelines for Systematic Quantification of Accuracy in Watershed
664 Simulations. *Transactions of the ASABE*, 50(3), 885–900. <https://doi.org/10.13031/2013.23153>

665

666 Murtaza, K. O., & Romshoo, S. A. (2016). Recent glacier changes in the Kashmir Alpine
667 Himalayas, India. <Http://Dx.Doi.Org/10.1080/10106049.2015.1132482>, 32(2), 188–205.
668 <https://doi.org/10.1080/10106049.2015.1132482>

669 Narsimlu, B., Gosain, A. K., & Chahar, B. R. (2013). Assessment of Future Climate Change
670 Impacts on Water Resources of Upper Sind River Basin, India Using SWAT Model. *Water
671 Resources Management*, 27(10), 3647–3662. <https://doi.org/10.1007/s11269-013-0371-7>

672 Nash, J. E., & Sutcliffe, J. v. (1970). River flow forecasting through conceptual models part I —
673 A discussion of principles. *Journal of Hydrology*, 10(3), 282–290. [https://doi.org/10.1016/0022-
1694\(70\)90255-6](https://doi.org/10.1016/0022-
674 1694(70)90255-6)

675 Praskievicz, S., & Chang, H. (2009). A review of hydrological modelling of basin-scale climate
676 change and urban development impacts: <Http://Dx.Doi.Org/10.1177/0309133309348098>, 33(5),
677 650–671. <https://doi.org/10.1177/0309133309348098>

678 Raftery, A. E., Gneiting, T., Balabdaoui, F., & Polakowski, M. (2005). Using Bayesian Model
679 Averaging to Calibrate Forecast Ensembles. *Monthly Weather Review*, 133(5), 1155–1174.
680 <https://doi.org/10.1175/MWR2906.1>

681 Räisänen, J., Hansson, U., Ullerstig, A., Döscher, R., Graham, L. P., Jones, C., Meier, H. E. M.,
682 Samuelsson, P., & Willén, U. (2004). European climate in the late twenty-first century: Regional
683 simulations with two driving global models and two forcing scenarios. *Climate Dynamics*, 22(1),
684 13–31. <https://doi.org/10.1007/S00382-003-0365-X/TABLES/1>

685 Raneesh, K. Y., & Santosh, G. T. (2011). A study on the impact of climate change on streamflow
686 at the watershed scale in the humid tropics. *Https://Doi.Org/10.1080/02626667.2011.595371*,
687 *56*(6), 946–965. <https://doi.org/10.1080/02626667.2011.595371>

688 Reshmidevi, T. v., Nagesh Kumar, D., Mehrotra, R., & Sharma, A. (2018). Estimation of the
689 climate change impact on a catchment water balance using an ensemble of GCMs. *Journal of*
690 *Hydrology*, *556*, 1192–1204. <https://doi.org/10.1016/J.JHYDROL.2017.02.016>

691 Rodrigues, J. A. M., Viola, M. R., Alvarenga, L. A., de Mello, C. R., Chou, S. C., de Oliveira, V.
692 A., Uddameri, V., & Morais, M. A. V. (2020). Climate change impacts under representative
693 concentration pathway scenarios on streamflow and droughts of basins in the Brazilian Cerrado
694 biome. *International Journal of Climatology*, *40*(5), 2511–2526.
695 <https://doi.org/10.1002/JOC.6347>

696 Romagnoli, M., Portapila, M., Rigalli, A., Maydana, G., Burgués, M., & García, C. M. (2017).
697 Assessment of the SWAT model to simulate a watershed with limited available data in the
698 Pampas region, Argentina. *The Science of the Total Environment*, *596–597*, 437–450.
699 <https://doi.org/10.1016/J.SCITOTENV.2017.01.041>

700 Romshoo, S. A., Dar, R. A., Rashid, I., Marazi, A., Ali, N., & Zaz, S. N. (2018). Implications of
701 Shrinking Cryosphere Under Changing Climate on the Streamflows in the Lidder Catchment in
702 the Upper Indus Basin, India. *Https://Doi.Org/10.1657/AAAR0014-088*, *47*(4), 627–644.
703 <https://doi.org/10.1657/AAAR0014-088>

704 Salathé, E. P. (2005). Downscaling simulations of future global climate with application to
705 hydrologic modelling. *International Journal of Climatology*, *25*(4), 419–436.
706 <https://doi.org/10.1002/JOC.1125>

707 Seager, R., & Vecchi, G. A. (2010). Greenhouse warming and the 21st century hydroclimate of
708 southwestern North America. *Proceedings of the National Academy of Sciences*, *107*(50),
709 21277–21282. <https://doi.org/10.1073/PNAS.0910856107>

710 Singh Jasrotia, A., Baru, D., Kour, R., Ahmad, S., & Kour, K. (2021). Hydrological modeling to
711 simulate stream flow under changing climate conditions in Jhelum catchment, western Himalaya.
712 *Journal of Hydrology*, *593*. <https://doi.org/10.1016/j.jhydrol.2020.125887>

713 Takele, G. S., Gebre, G. S., Gebremariam, A. G., & Engida, A. N. (2021). Hydrological modeling
714 in the Upper Blue Nile basin using soil and water analysis tool (SWAT). *Modeling Earth*
715 *Systems and Environment*. <https://doi.org/10.1007/s40808-021-01085-9>

716 Tan, M. L., Ibrahim, A. L., Yusop, Z., Chua, V. P., & Chan, N. W. (2017). Climate change
717 impacts under CMIP5 RCP scenarios on water resources of the Kelantan River Basin, Malaysia.
718 *Atmospheric Research*, *189*, 1–10. <https://doi.org/10.1016/j.atmosres.2017.01.008>

719 Taylor, K. E. (2001). Summarizing multiple aspects of model performance in a single diagram.
720 *Journal of Geophysical Research: Atmospheres*, 106(D7), 7183–7192.
721 <https://doi.org/10.1029/2000JD900719>

722 Taylor, K. E., Stouffer, R. J., & Meehl, G. A. (2012). An Overview of CMIP5 and the
723 Experiment Design. *Bulletin of the American Meteorological Society*, 93(4), 485–498.
724 <https://doi.org/10.1175/BAMS-D-11-00094.1>

725 Teutschbein, C., & Seibert, J. (2012). Bias correction of regional climate model simulations for
726 hydrological climate-change impact studies: Review and evaluation of different methods.
727 *Journal of Hydrology*, 456–457, 12–29. <https://doi.org/10.1016/J.JHYDROL.2012.05.052>

728 Touseef, M., Chen, L., & Yang, W. (2021). Assessment of surfacewater availability under
729 climate change using coupled SWAT-WEAP in hongshui river basin, China. *ISPRS*
730 *International Journal of Geo-Information*, 10(5). <https://doi.org/10.3390/ijgi10050298>

731 Uniyal, B., Jha, M. K., & Verma, A. K. (2015). Assessing Climate Change Impact on Water
732 Balance Components of a River Basin Using SWAT Model. *Water Resources Management*,
733 29(13), 4767–4785. <https://doi.org/10.1007/s11269-015-1089-5>

734 Uusitalo, L., Lehikoinen, A., Helle, I., & Myrberg, K. (2015). An overview of methods to
735 evaluate uncertainty of deterministic models in decision support. *Environmental Modelling &*
736 *Software*, 63, 24–31. <https://doi.org/10.1016/J.ENVSOFT.2014.09.017>

737 van den Hurk, B., Hirschi, M., Schär, C., Lenderink, G., van Meijgaard, E., van Ulden, A.,
738 Rockel, B., Hagemann, S., Graham, P., Kjellström, E., & Jones, R. (2005). Soil Control on
739 Runoff Response to Climate Change in Regional Climate Model Simulations. *Journal of*
740 *Climate*, 18(17), 3536–3551. <https://doi.org/10.1175/JCLI3471.1>

741 Vetter, T., Reinhardt, J., Flörke, M., van Griensven, A., Hattermann, F., Huang, S., Koch, H.,
742 Pechlivanidis, I. G., Plötner, S., Seidou, O., Su, B., Vervoort, R. W., & Krysanova, V. (2017).
743 Evaluation of sources of uncertainty in projected hydrological changes under climate change in
744 12 large-scale river basins. *Climatic Change*, 141(3), 419–433. [https://doi.org/10.1007/s10584-](https://doi.org/10.1007/s10584-016-1794-y)
745 [016-1794-y](https://doi.org/10.1007/s10584-016-1794-y)

746 Viviroli, D., Dürr, H. H., Messerli, B., Meybeck, M., & Weingartner, R. (2007). Mountains of the
747 world, water towers for humanity: Typology, mapping, and global significance. *Water Resources*
748 *Research*, 43(7). <https://doi.org/10.1029/2006WR005653>

749 Vogel, R. M., Stedinger, J. R., Batchelder, R., & Lee, S. U. (2008). Appraisal of the Generalized
750 Likelihood Uncertainty Estimation (GLUE) Method. *World Environmental and Water Resources*
751 *Congress 2008: Ahupua'a - Proceedings of the World Environmental and Water Resources*
752 *Congress 2008*, 316, 1–10. [https://doi.org/10.1061/40976\(316\)611](https://doi.org/10.1061/40976(316)611)

753 Wallach, D., Mearns, L. O., Ruane, A. C., Rötter, R. P., & Asseng, S. (2016). Lessons from
754 climate modeling on the design and use of ensembles for crop modeling. *Climatic Change*,
755 *139*(3–4), 551–564. <https://doi.org/10.1007/S10584-016-1803-1/TABLES/1>

756 Yu, Z., Gu, H., Wang, J., Xia, J., & Lu, B. (2018). Effect of projected climate change on the
757 hydrological regime of the Yangtze River Basin, China. *Stochastic Environmental Research and*
758 *Risk Assessment*, *32*(1). <https://doi.org/10.1007/s00477-017-1391-2>

759 Zhang, H., & Huang, G. H. (2013). Development of climate change projections for small
760 watersheds using multi-model ensemble simulation and stochastic weather generation. *Climate*
761 *Dynamics*, *40*(3–4), 805–821. <https://doi.org/10.1007/S00382-012-1490-1/FIGURES/4>

762

763

764

765

766

767

768

769

770

771

772

773

774

775

776

777

778

779

780

781

782

783

Conflict of interest

784

785 The authors declare that there is no conflict of financial or personal interests or beliefs that could
786 affect the objectivity of this research.

787

788 **Akhtar Alam**

789 On behalf of all authors

790

791

792

Data Availability Statement

793 The datasets generated during and/or analysed during the current study are available from the
794 corresponding author on reasonable request.

795 **Akhtar Alam**

796 On behalf of all authors

797

798

799

Author Contributions Statement

800 Shafkat Ahsan has been primary involved in modelling part and writing; M. Sultan Bhat
801 developed the idea and contributed in writing; Akhtar Alam performed some simulations,
802 contributed in writing and overall editing of the manuscript; Hakim Farooq coordinated the work
803 and was responsible for literature review and compilation of the results; and Hilal A. Sheikh did
804 the artwork.

805

806

807

808 **Akhtar Alam**

809 On behalf of all authors

810

811

812

813

814

Figures

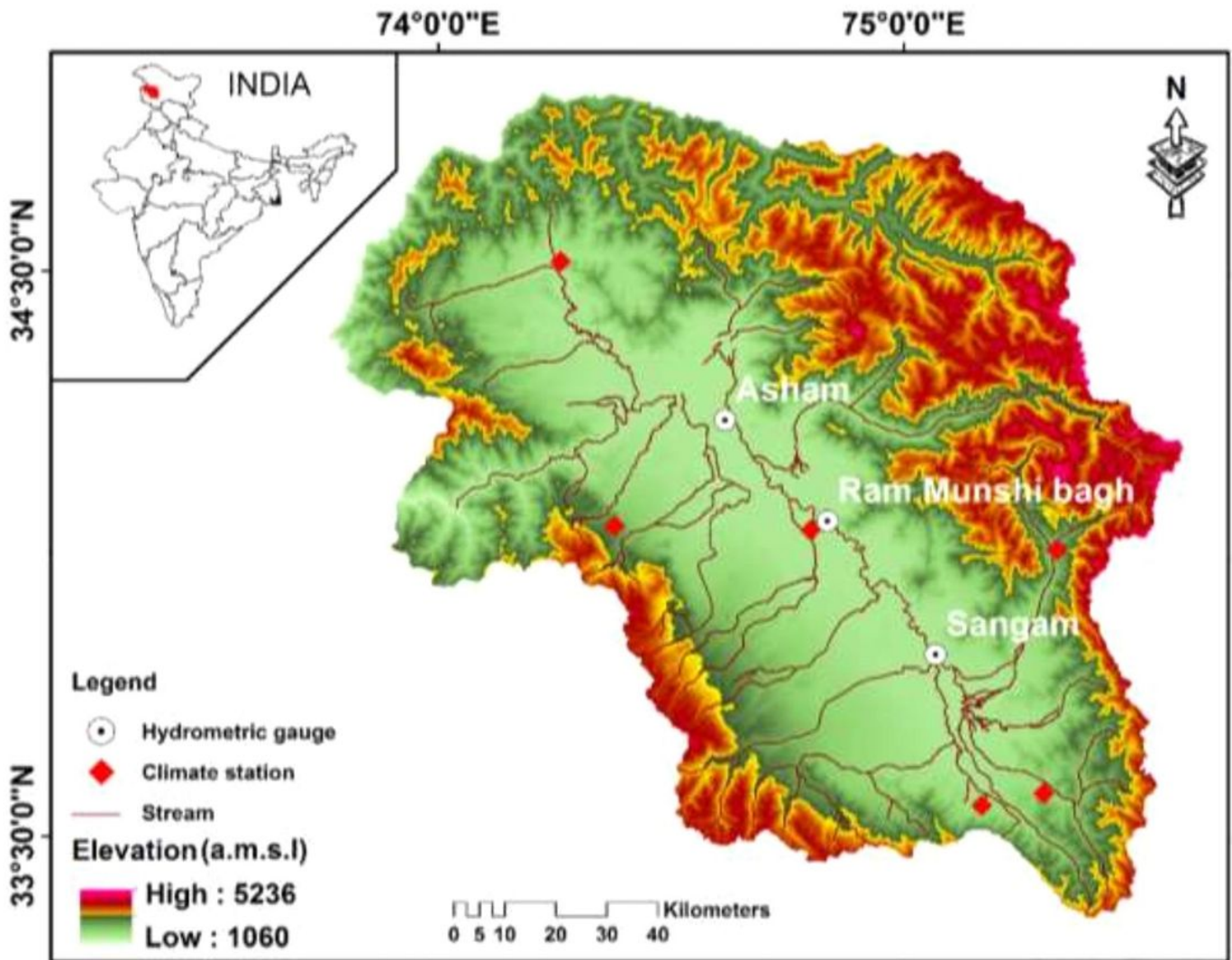


Figure 1

Location map of the Jhelum basin with the major streams, climatic stations and the river gauges.

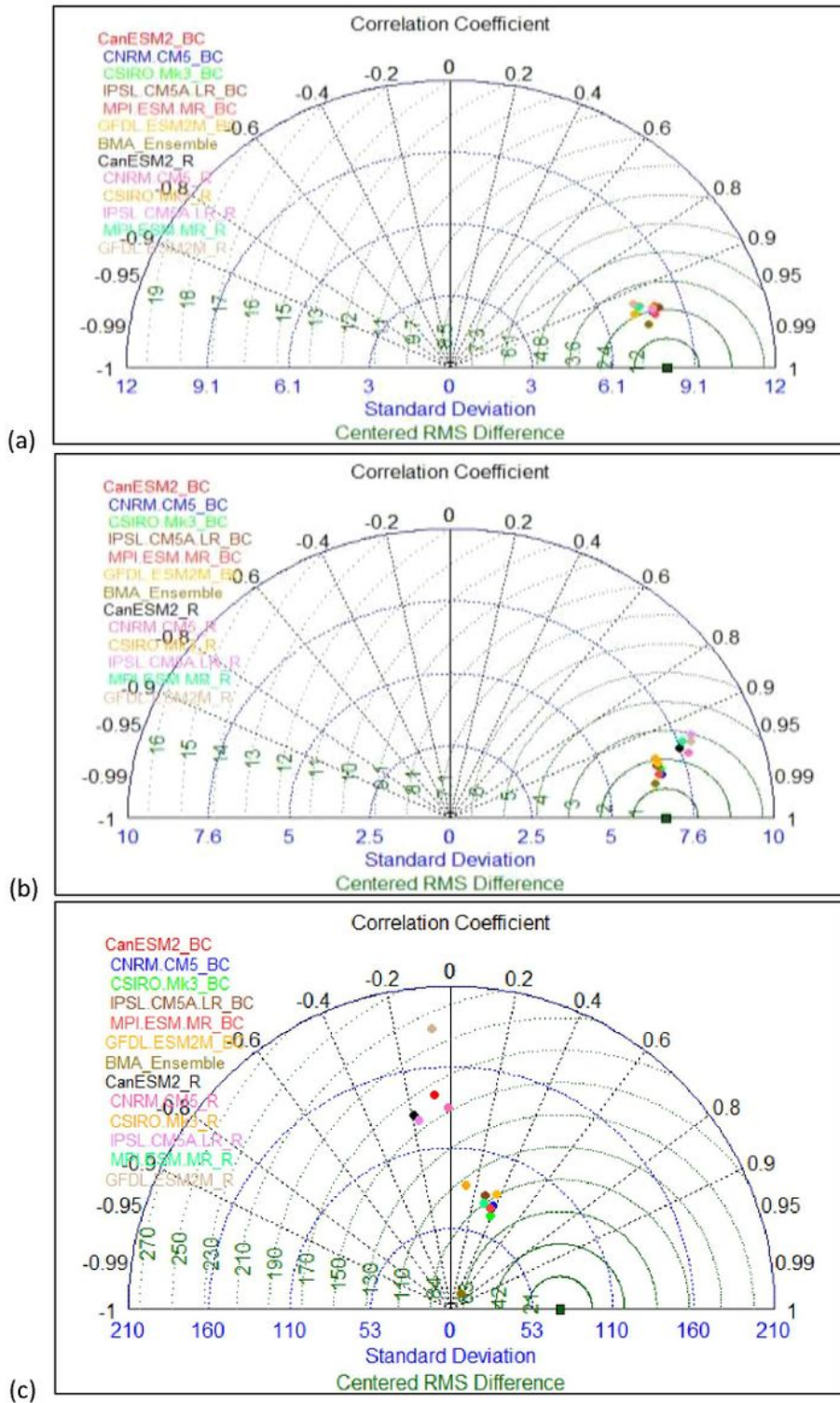


Figure 2

Performance of GCMs and BMA ensemble during training period (1980-2005); (a) mean maximum temperature, (b) mean minimum temperature and (c) precipitation. BC = bias corrected GCM output, R= raw GCM output.

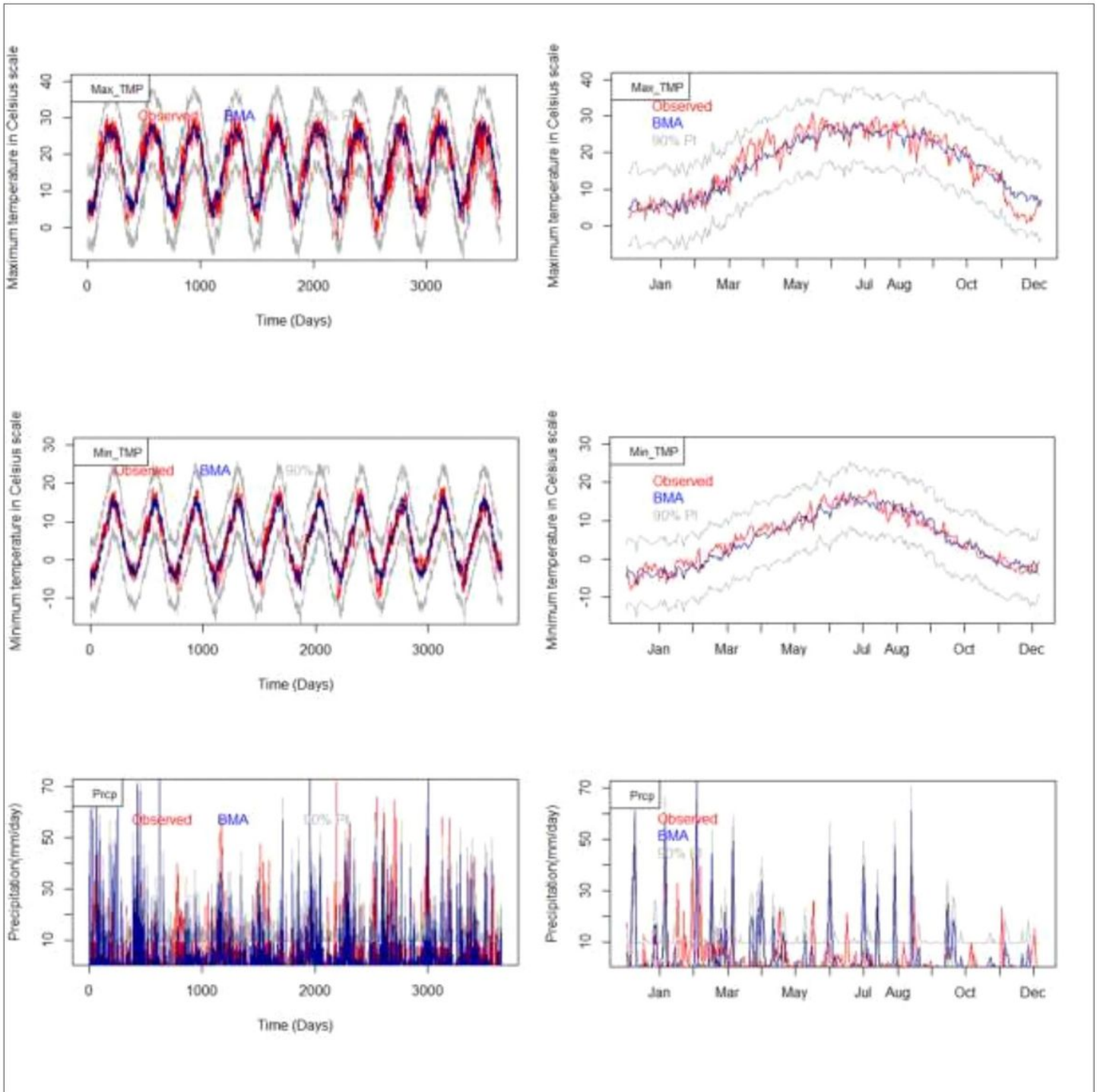


Figure 3

Performance of the BMA during training period, left - daily data for 10yrs and right - data for only 1yr for detailed visualization. Max_TMP = mean maximum temperature, Min_TMP = mean minimum temperature, and Prcp = Precipitation.

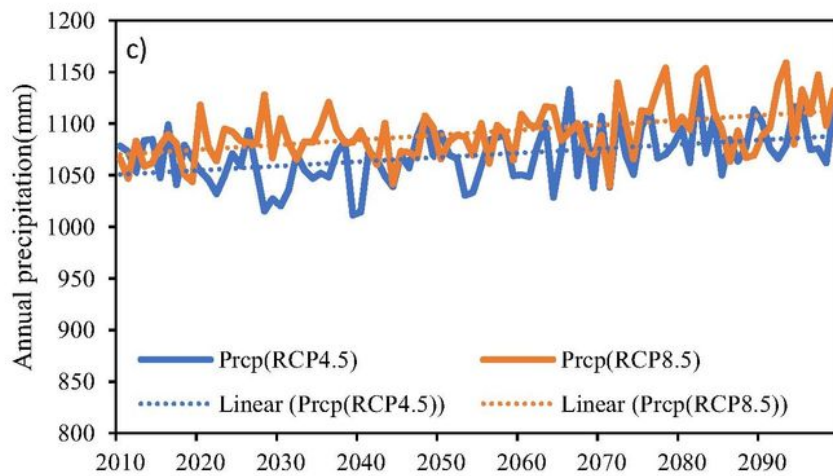
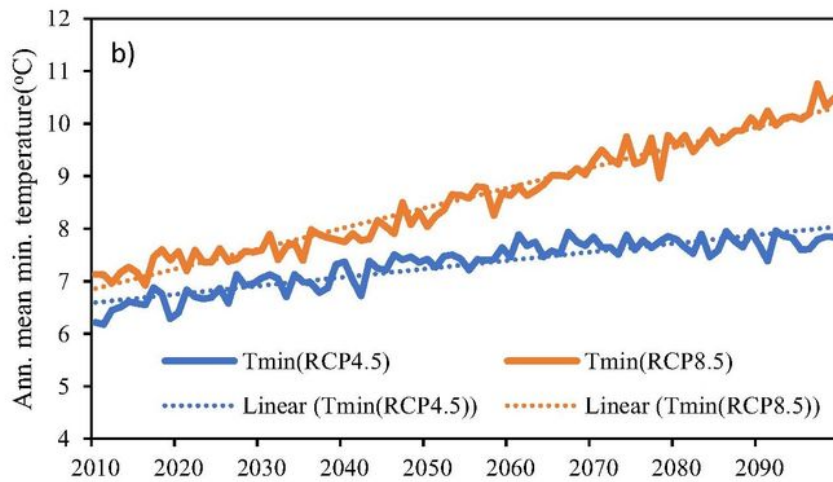
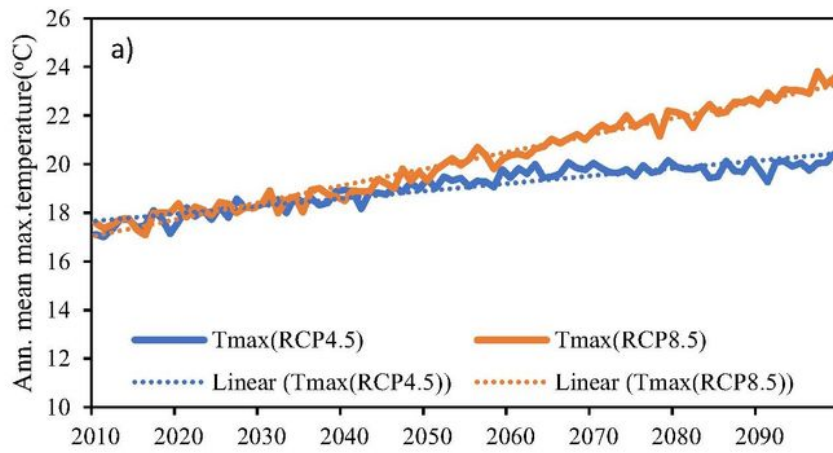


Figure 4

BMA based projected changes in annual mean maximum temperature (a), mean minimum temperature (b), and precipitation (c) under RCP4.5 and RCP8.5, with respect to the baseline (1980-2010) values for Jhelum basin.

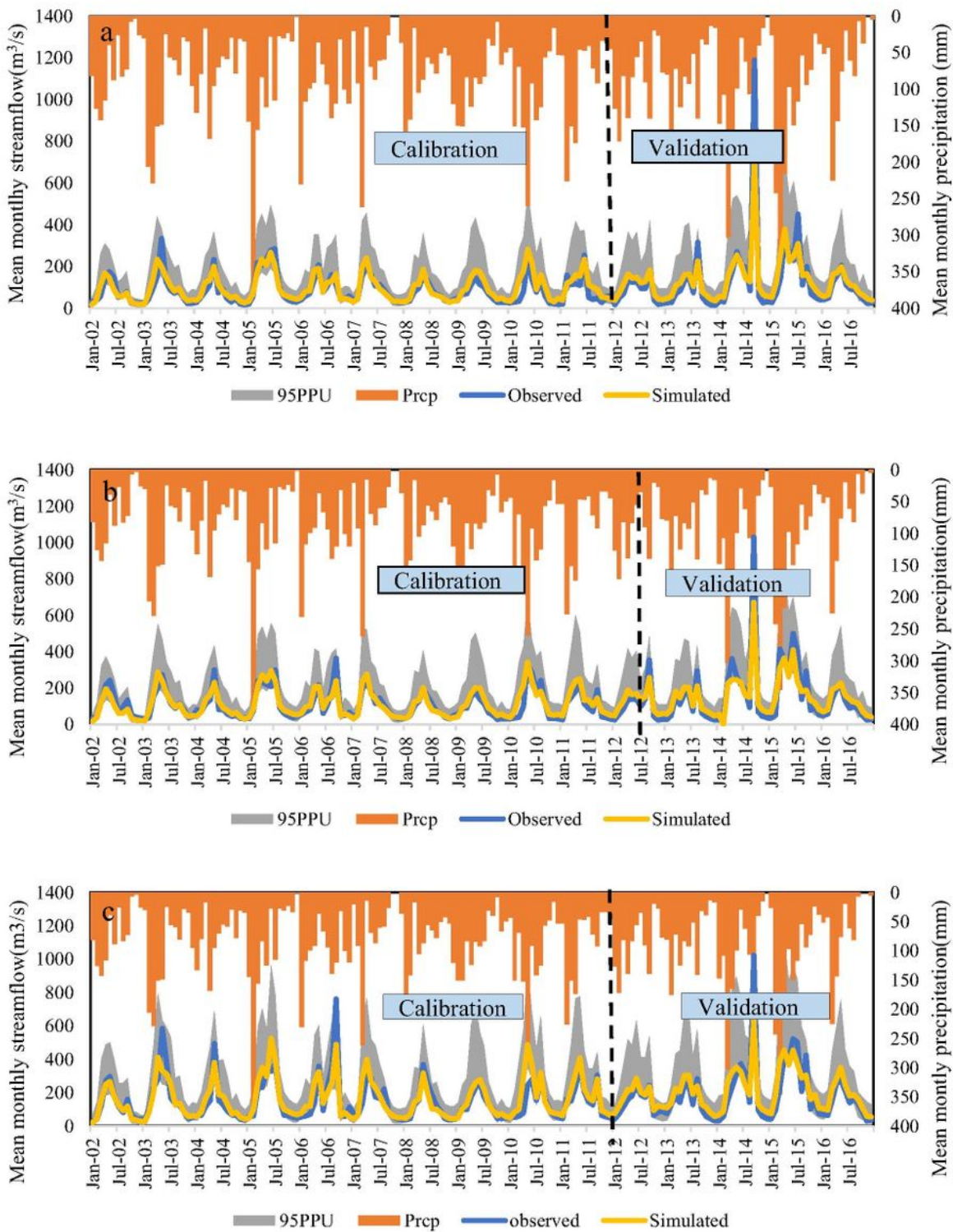


Figure 5

Multi-site evaluation of the SWAT model during calibration (2002-2011) and validation (2012-2016) periods at Sangam gauge (a), Ram Munshi Bagh gauge (b) and Asham gauge (c) stations.

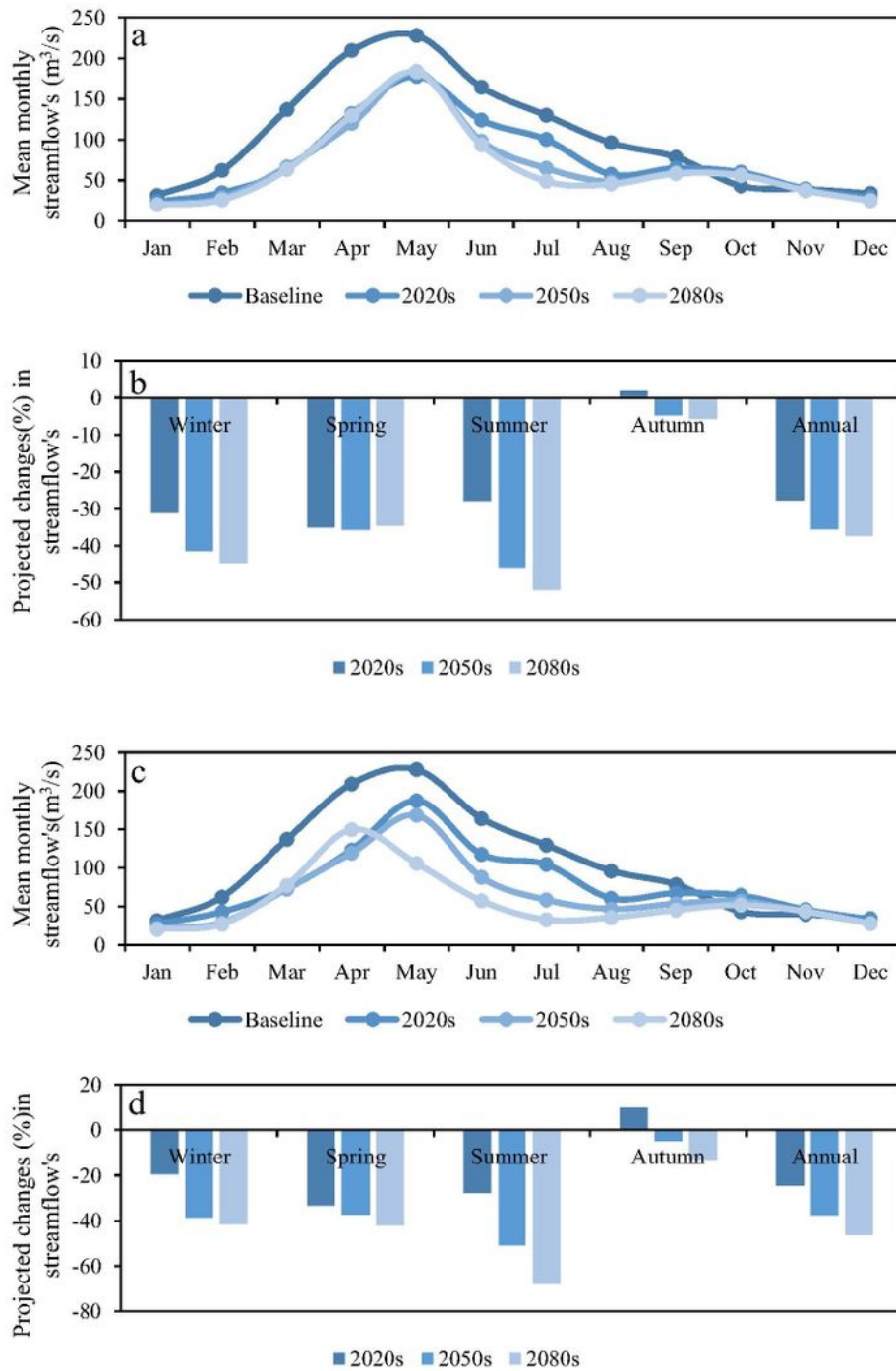


Figure 6

Projected changes in mean monthly and seasonal streamflow of Jhelum at Sangam gauge under RCP4.5 (a, b) and RCP8.5 (c, d) over 21st century

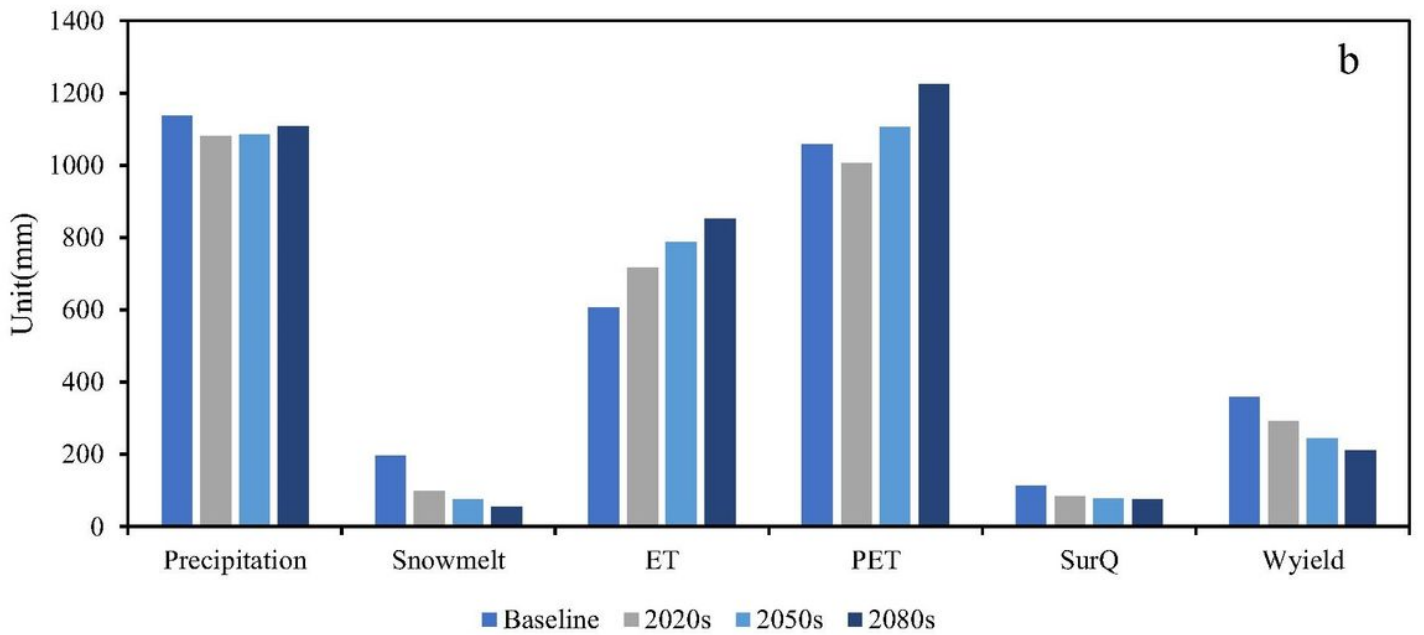
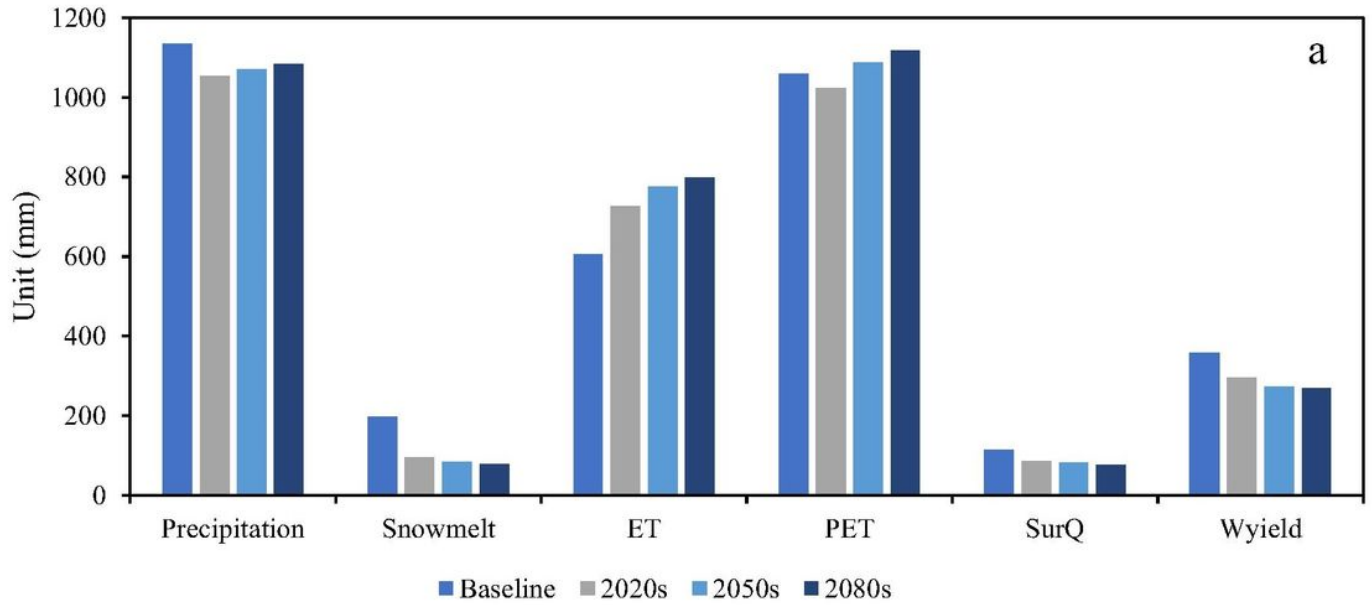


Figure 7

Projected changes in the annual average water balance components of the Jhelum basin under RCP4.5 (a) and RCP8.5 (b) over 21st century.

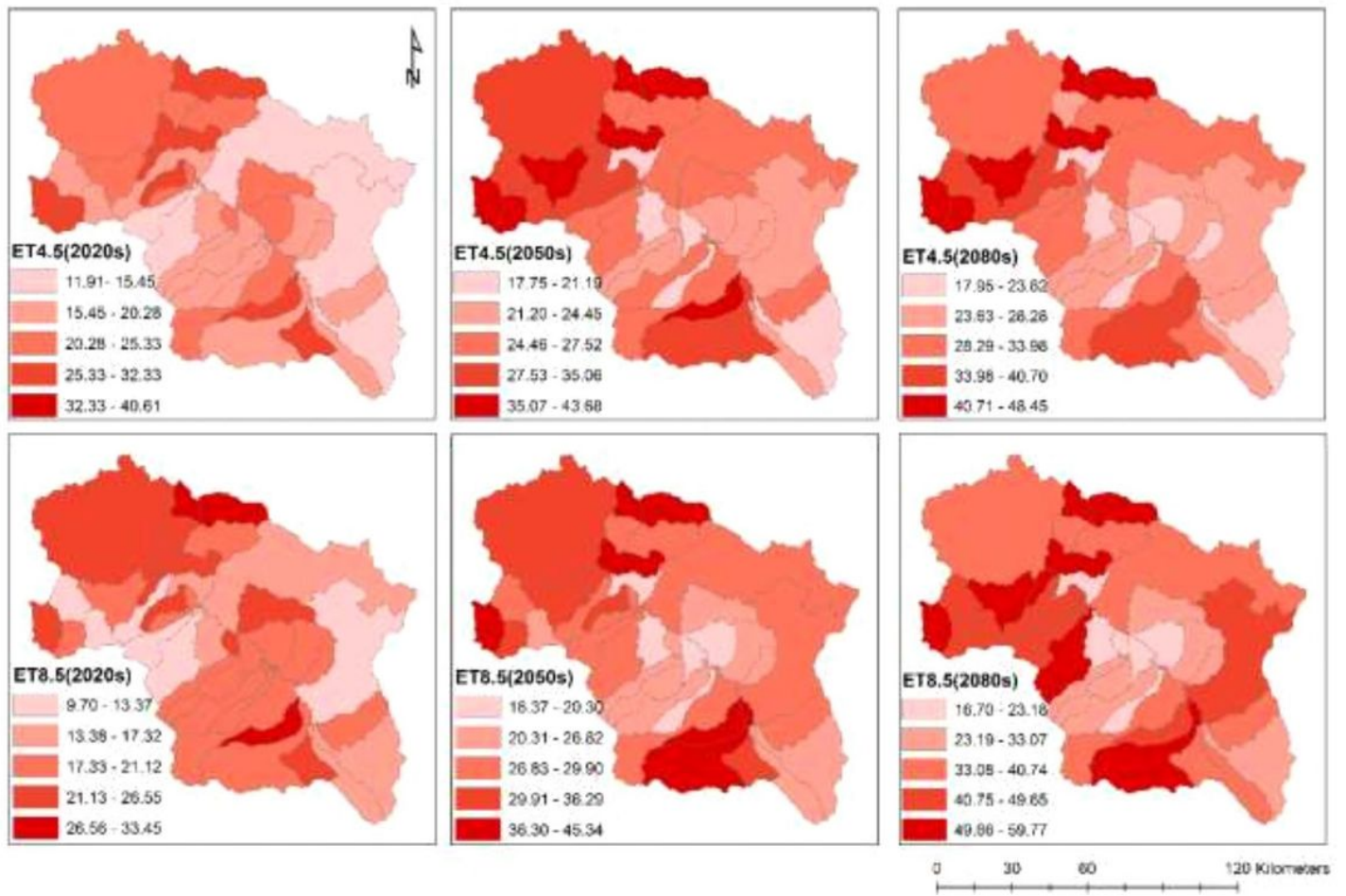


Figure 8

Spatial distribution of the projected changes (%) in evapotranspiration of the Jhelum basin under RCP4.5 (top) and RCP8.5 (bottom).

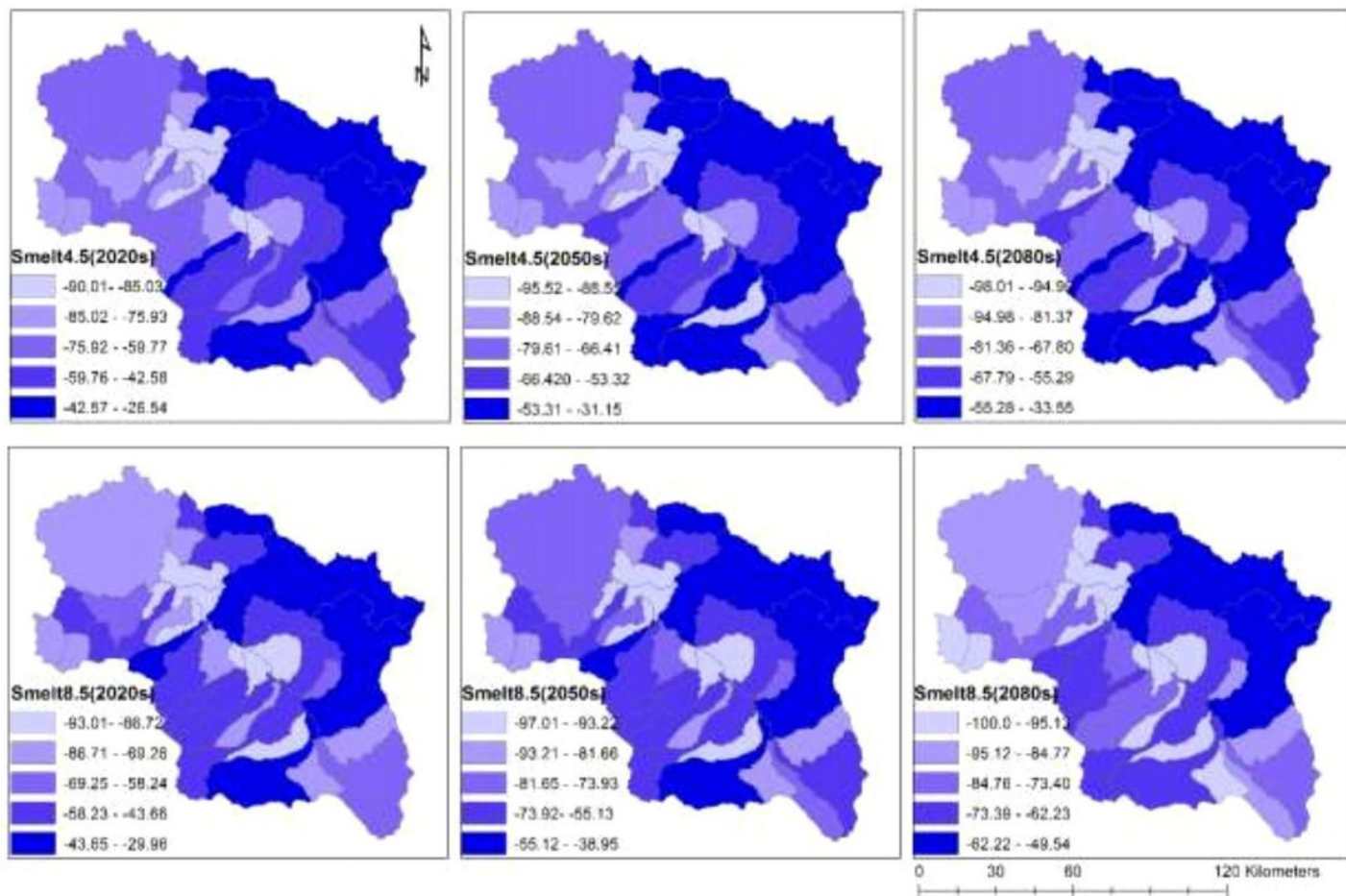


Figure 9

Spatial distribution of the projected changes (%) in the snowmelt of the Jhelum basin under RCP4.5 (top) and RCP8.5 (bottom)

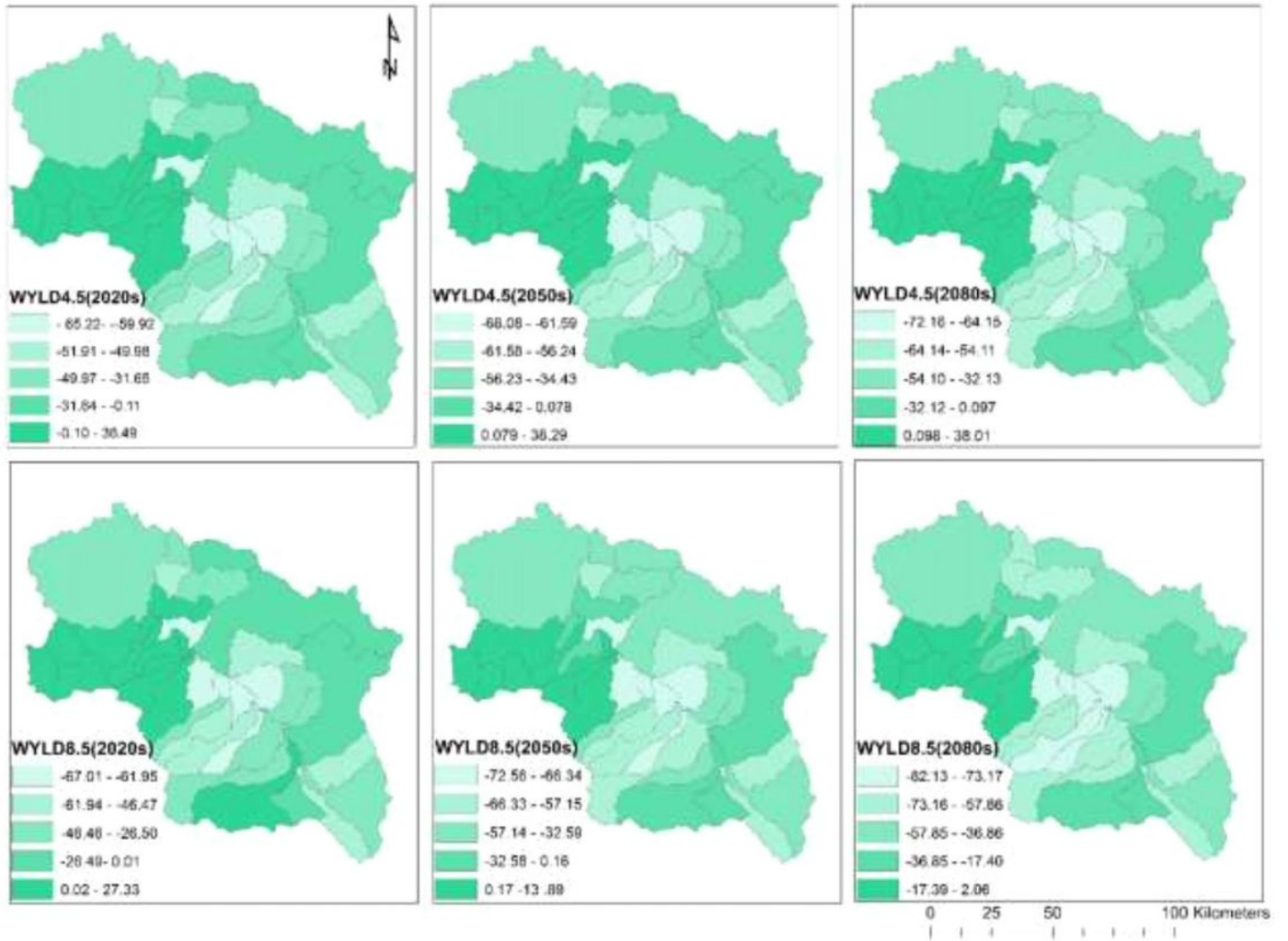


Figure 10

Spatial distribution of the projected changes (%) in the water yield of the Jhelum basin under RCP4.5 (top) and RCP8.5 (bottom).